Resilient Design Coalition RDC

SPEEDCORE FUNCTIONAL RECOVERY PREQUALIFICATION

Complete Draft Report Submitted for Peer-Review

CHARLES PANKOW FOUNDATION
Building Innovation through Research

kpff

UBC

SP3 Seismic Performance Prediction Platform by Haselton Baker Risk Group

RESILIENT DESIGN FOR FUNCTIONAL RECOVERY: PREQUALIFICATION REPORT FOR SPEEDCORE WALLS

Complete Draft Report Submitted for Peer-Review

Prepared By:

Resilient Design Coalition

Financially Supported by:

American Institute of Steel Construction and the Charles Pankow Foundation

WORKING GROUP MEMBERS:

Ed Almeter, MS
Kristen Blowes, PhD, PE
Jared DeBock, PhD, PE
Curt Haselton, PhD, PE
Carlos Molina Hutt, PhD, PE
Huy Pham, PhD
David Welch, PhD
Reid Zimmerman, SE

August 8, 2025

QUANTIFICATION OF FUNCTIONAL RECOVERY SEISMIC PERFORMANCE FACTORS FOR THE SPEEDCORE SYSTEM

Submitted: 08/08/2025

EXECUTIVE SUMMARY

This report documents the quantification of the functional recovery seismic performance factors for the uncoupled and coupled configurations of the SpeedCore (composite plate shear walls—concrete filled) system. Quantification of the functional recovery seismic performance factors is performed in accordance with the proposed Section A.8 procedures of the 2026 National Earthquake Hazards Reduction Program (NEHRP) Provisions. The functional recovery seismic performance factors include the functional recovery response modification coefficient, $R_{fr,}$, and functional recovery allowable story drift limit, $\Delta_{afr.}$ These were determined by developing an archetype space of different building heights, designed with various functional recovery response modification coefficients and allowable drift limits, and then selecting the combination that results in less than a 10% mean probability of Safety-Critical Structural Damage, or P[SCSD], in each performance group, and less than 20% P[SCSD] for any individual archetype, for Functional Recovery Category (FRC) A, B and C. The 10% and 20% thresholds are modified to 15% and 25%, respectively, for FRC D. All analyses are conducted at the Functional Recovery Earthquake (FRE_R) level shaking corresponding to a Seismic Design Category $D_{max,FRE}$ condition with two-point spectral ordinates S_{dsfr} and S_{d1fr} of 1.25 and 0.75, respectively.

The proposed R_{fr} and Δ_{afr} for SpeedCore are presented in the table below. Results demonstrate the difference in R_{fr} between uncoupled and coupled configurations. At first glance, this appears non-intuitive since coupled SpeedCore configurations are permitted a higher R in ASCE 7 Chapter 12 than uncoupled configurations. While coupling beam hinging exhibits high ductility and is desirable from a collapse prevention perspective, the results of this study show that early coupling beam damage requires repairs to achieve functional recovery. Hence, a lower R_{fr} value is necessary for coupled SpeedCore configurations. It should be noted that proposed R_{fr} values for coupled SpeedCore configurations are sensitive to coupling beam geometry, particularly coupling beam length.

Table 1 – Proposed design criteria to satisfy the Functional Recovery performance objectives for SpeedCore systems

	FRC A/B/C		FRC D	
System	$\mathbf{R_{fr}}$	$\mathbf{\Delta_{afr}}$	$\mathbf{R_{fr}}$	$\mathbf{\Delta_{afr}}$
SpeedCore Coupled*	5.5	0.75%	6.5	0.75%
SpeedCore Uncoupled	4.5	1.00%	5.0	1.00%

*Applicable to coupled SpeedCore systems with coupling beam lengths greater than or equal to 7.5ft in length

Contents

1.

2. INTRODUCTION

This report documents the quantification of the functional recovery seismic performance factors for the uncoupled and coupled configurations of the SpeedCore (composite plate shear walls—concrete filled) system. Quantification of the functional recovery seismic performance factors is performed in accordance with the proposed Section A.8 procedures of the 2026 National Earthquake Hazards Reduction Program (NEHRP) Provisions. The functional recovery seismic performance factors include the functional recovery response modification coefficient, $R_{fr,}$, and functional recovery allowable story drift limit, $\Delta_{afr.}$ These are the equivalents of the response modification coefficient, R, and allowable story drift limit, Δ_a, used in ASCE/SEI 7 Chapter 12 but for design for functional recovery.

An archetype space of different building heights, designed with various functional recovery response modification coefficients and allowable drift limits was developed. FEMA P-58/ATC-138 (FEMA, 2018a; ATC, 2021) models were then created. In accordance with the proposed Section A.8 procedures of the 2026 NEHRP Provisions, only structural components are included in these FEMA P-58/ATC-138 performance models. Design of the archetypes was performed using the automated design capability of SP3 (www.sp3risk.com) and engineering demand parameters (e.g., story drift ratios, wall chord rotations, coupling beam rotations, etc.) were estimated using SP3's Response Prediction Engine, which while calibrated based on extensive nonlinear response history analyses, does not perform nonlinear response history analyses of the specific archetype directly.

Performance assessments of each model are conducted following FEMA P-58 (FEMA, 2018a) and ATC-138 recommendations to quantify the probability of safety-critical structural damage (P[SCSD]) for each archetype (Blowes et al., in review). The triggering of SCSD is governed by the assigned safety class for a given component and damage state according to the ATC-138 methodology. The safety class controls what percentage of components, in each story and direction, that can be in each damage state or greater, prior to triggering SCSD in the building. The P[SCSD] serves as an acceptable proxy for the probability of exceeding the target functional recovery times for structural-only models, as outlined in section CA.8.3.5 of the 2026 NEHRP Seismic Provisions.

The functional recovery seismic performance factors are selected such that archetypes designed for that R_{fr} and Δ_{afr} result in less than a 10% mean P[SCSD] in each performance group and less than 20% P[SCSD] for any individual archetype for Functional Recovery Category (FRC) A, B and C. The 10% and 20% are modified to 15% and 25%, respectively, for FRC D. These limits are in accordance with the proposed Section A.8 procedures of the 2026 National Earthquake Hazards Reduction Program (NEHRP) Provisions. All analyses are conducted at the Functional

Recovery Earthquake (FRE_R) level shaking corresponding to a Seismic Design Category $D_{max,FRE}$ condition with two-point spectral ordinates S_{dsfr} and S_{d1fr} of 1.25 and 0.75, respectively.

3. ANALYSIS METHODS

The methods used to perform the functional recovery analyses are presented in this section. Discussion of performing design iterations and acceptance criteria for the SpeedCore system are discussed in Section 3.1. Background information on the fragility functions used to estimate SCSD is provided in Section 3.2. The details of the archetype design space used for analysis are provided in Section 3.3. The estimation of structural responses, or engineering demand parameters (EDPs), is discussed in Section 3.4.

3.1. Design Iteration and Acceptance Criteria for Seismic Performance Factors

For each individual archetype, design iterations are carried out using values of R_{fr} and Δ_{afr} across the ranges of 1 through R (i.e., up to the response modification coefficient used in life-safety design) and 0.5% through 2.0% (i.e., up to the maximum allowable story drift ratio for Risk Category II structures), respectively. The Response Modification Factor, R, is 6.5 and 8 for uncoupled and coupled SpeedCore systems, respectively, in accordance with Table 12.2-1 of ASCE 7-22 (ASCE, 2022). These design iterations are performed using the SP3 design engine that estimates strength and stiffness of each design to estimate appropriate structural responses and subsequent estimates of SCSD.

In each performance group, the combination of R_{fr} and Δ_{afr} is deemed to be acceptable if the mean P[SCSD] is less than 10%, and the maximum P[SCSD] across all archetypes in the performance group is less than 20% for quantifying the functional recovery seismic performance factors for Functional Recovery Category (FRC) A, B and C. For FRC D, the mean and maximum P[SCSD] across all archetypes in a performance group must be less than 15% and 25%, respectively. The recommended design values for a particular system are taken as the most restrictive across all performance groups, rounded to the nearest increment considered (0.5 for R_{fr} and 0.25% for Δ_{afr}).

The requirements of the proposed Section A.8 procedures of the 2026 NEHRP Provisions impose that R_{fr} and Δ_{afr} shall not be taken less than R/1.5 and 1% for FRC A, B and C and R/1.25 and 1.5% for FRC D. These "judgment-based" upper limits on seismic performance factors correspond to values required for Risk Category IV (FRC A, B, and C) and Risk Category III (FRC D) structures when performing life safety design. Additionally, to verify the strength and stiffness coupling inherent to each design variant, each archetype model is re-assessed under an independent strength and stiffness assumption, i.e., where additional strength prescribed by R_{fr} does not add additional stiffness to the building. Analysis outcomes from the independent-strength-and-stiffness assessment are checked to ensure the maximum P[SCSD] does not exceed the acceptance criteria (20% for FRC A/B/C and 25% for FRC D), where applicable. The judgment-based upper limit and the independent-strength-and-stiffness check provide a reasonable limit, preventing too great a reliance on the analytical results and recognizing the historical precedent set by the higher Risk Categories.

3.1.1. Safety-Critical Structural Damage (SCSD)

The triggering of SCSD is governed by the assigned safety class for a given component and damage state according to the ATC-138 methodology (ATC, 2021). The safety class controls the percent of components, in each story and direction, that can be in each damage state or greater, prior to triggering SCSD. A summary of the ATC-138 safety class descriptions and acceptance thresholds is shown in Table 2.

Table 2. ATC-138 safety-class definitions for triggering SCSD (ATC, 2021).

Safety Class	Description	Acceptance Threshold[a]
0	Slight damage that is not a safety concern and will never trigger an unsafe placard	N/A
1	Moderate damage that may be visually concerning, but does not substantially reduce the lateral strength of the component.	50%
2	Severe damage that causes substantial loss of lateral strength of the component, but does not substantially reduce its vertical load carrying capacity.	25%
3	Severe damage that compromises both lateral and vertical load carrying capacity of the component.	10%

[a] Percentages reflect the upper quantity of components, in each story and direction, that can be in a safety class of interest before triggering safety-critical structural damage (SCSD)

3.1.2. System Specific SCSD Considerations

The three main groups of components that are considered for SpeedCore building SCSD assessment are the walls, the coupling beams (for coupled systems), and the steel frame gravity system. The specific components and damage state safety class assignments are discussed in Section 3.2.

Unlike the other components that can cause SCSD, the coupling beam safety class thresholds were considered at a building-level rather than a story-level. The key distinction is that the safety class threshold is applied across the entire height of the building per direction, instead of per-story and per-direction. This was done in this manner because the coupling beams act together to resist lateral loads up the entire height of the building, not at a single level, so coupling beam failures at a single level (with no other coupling beam damage over the building height) does not result in a stability or substantial strength loss issue; for coupling beams to cause substantial lateral strength loss (to warrant triggering of SCSD), the coupling beams need to be damaged over multiple stories), so triggering SCSD for damage on a single level would be inappropriate for coupling beams. This assumes that the walls remain intact enough to allow the transfer of loads between levels, which is reasonable because the damage occurs primarily at the base of the wall, not up the height of the building. The difference in this building-level vs. story-level distinction can be illustrated with the extreme case of significant damage to just one of the two coupling beams in a given story and direction while the remainder of the coupling beams in the building remain intact. In the per-story approach, the percent of damaged components would be 50% and that would trigger SCSD for the entire building (assuming SC2 for the coupling beam damage state). In the building-level approach, the percent damage would be [100/N]% (where N is the number of stories) so for anything over 4 stories safety class 2 would not trigger SCSD.

3.2. Fragility Functions for the SpeedCore System

Fragility functions are used to relate structural responses to likely damage and consequences. Fragility functions are commonly modeled by a lognormal distribution defined by a lognormal mean (θ) and standard deviation (β). For a given structural component, sequential damage states (DSs) can be represented by individual fragility functions that represent the likelihood of a distinct level of damage and corresponding level of repair effort and consequences. Additionally, damage states may be mutually exclusive, where a single fragility function may be used to represent multiple outcomes (i.e., sub-damage states) where the likelihood of each is given a weighting that sums to unity (e.g., 0.25 + 0.75 = 1). The fragility functions used in the current study will use both sequential and mutually exclusive damage state definitions. More general background information on fragility functions and damage state development can be found in FEMA P-58-1 (FEMA, 2018a).

The following sub-sections provide details on the structural component fragility functions, including:

- SpeedCore walls;
- SpeedCore coupling beams (for coupled systems only);
- Steel gravity framing beam-to-column connections (for both uncoupled and coupled systems).

3.2.1. SpeedCore Wall Fragilities

SpeedCore wall fragilities were developed within a previous study conducted for AISC (Welch et al. 2024). The fragility development is based on experimental testing conducted at SUNY

Buffalo and Purdue University. A total of twelve wall specimens were used for fragility development. The configurations included planar rectangular walls, planar walls with circular HSS boundaries, C-shaped walls, and T-shaped walls. A summary of the experimental studies is provided in Table 3.

Table 3. Experimental testing used for SpeedCore wall fragility development (Welch et al. 2024).

References	Assembly Type	Specimen
Shafaei et al. (2020); Shafaei et al. (2021)	Planar Wall - Rectangular	CW-42-55-10-T
		CW-42-55-20-T
		CW-42-55-30-T
		CW-42-14-20-T
		CW-42-14-20-TS
Alzeni and Bruneau (2014);	Planar Wall – HSS Cap	NB1
Alzeni and Bruneau (2017)	Planar Wall – HSS BE	B1
Kenarangi et al. (2020); Kenarangi et al. (2021)	C-Shaped Wall	C1
		C2
Kizilarslan et al. (2021a); Kizilarslan and Bruneau (2023a)	T-Shaped Wall	T2
		T3
		T4

Table 4. SpeedCore wall fragility damage states and corresponding safety classes.

Damage State	Median (θ)[a]	β	Safety Class[b]	Damage Description	Repair Measures
DS1	1.64%	0.36	1	Yielding, visible buckling, onset of weld or plate fracture	Cut out fractured and buckled regions, inspect and repair concrete as needed, reinforce ends of wall with repair plate, repair slab finish as needed.
DS2	2.32%	0.35	2	Severe distributed buckling, fracture propagation through flanges/webs, tie-bar weld failure, concrete crushing	Remove badly damaged plate sections, inspect and replace damaged concrete, replace damaged or removed tie-bars as applicable, re-weld new plate around base of wall, replace slab finish as needed.

[a] Fragility function is a lognormal distribution with median and standard deviation of θ and β, respectively. The EDP is wall chord rotation.
[b] SC 1 = 50%, SC 2 = 25%, SC 3 = 10% allowable quantity of damaged components per direction per story; SC 0 does not result in SCSD.

Fragility development used wall chord rotation as an EDP, which was defined as the global drift response of the entire wall assembly during testing. FEMA P-58-1 Appendix H (FEMA, 2018a) was followed when developing the fragility functions. The fragility functions for SpeedCore wall assemblies are comprised of two sequential damage states (DS). DS1 is closely associated with displacement demands corresponding to peak strength, while DS2 is closely associated with significant strength loss (i.e., >20% strength loss from peak resistance).

A summary of the SpeedCore wall fragility functions and corresponding safety class assignments is provided in Table 4. Figure 1 shows example photographs of each damage state. A plot of the fragility functions is provided in Figure 2. Additional details of SpeedCore wall fragility development can be found in Welch et al. (2024).

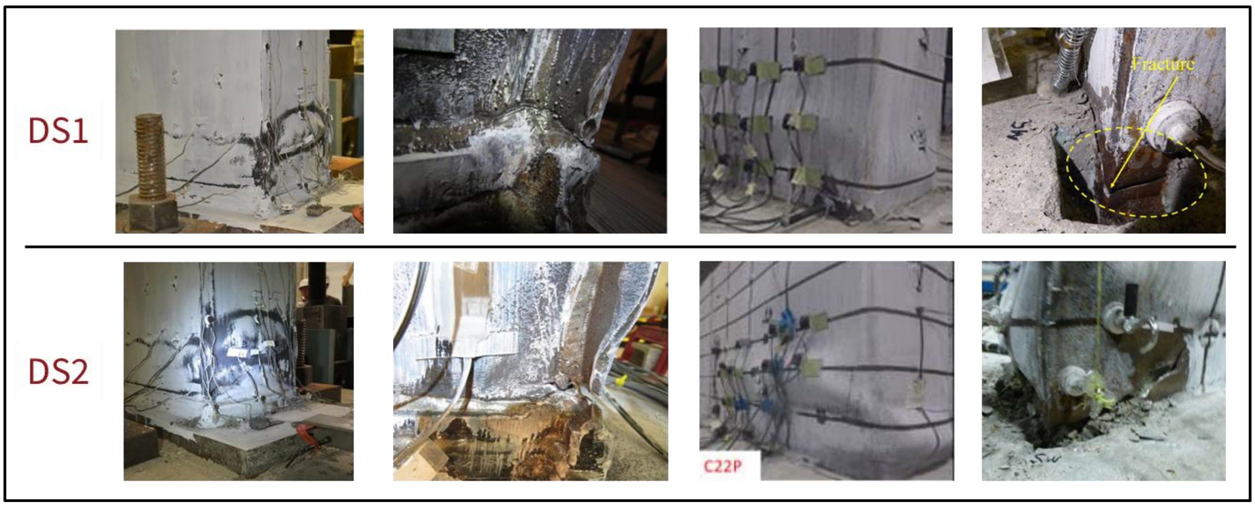

Figure 1. Examples of damage states for SpeedCore wall assemblies (Welch et al. 2024).

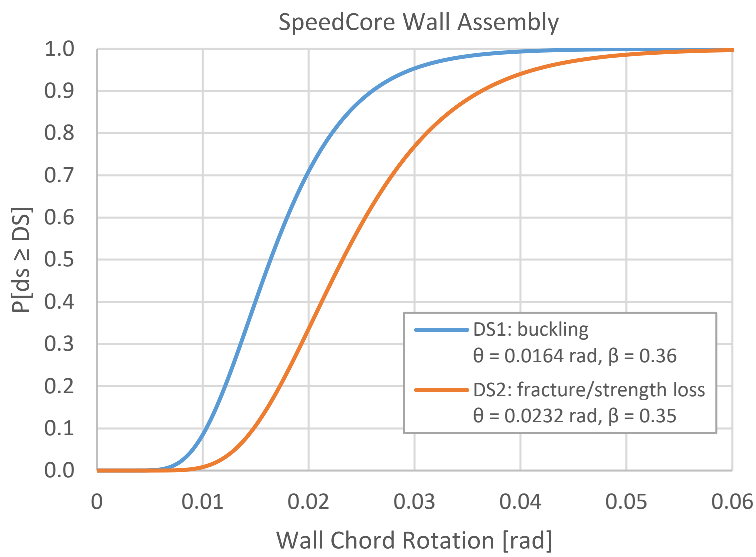

Figure 2. Fragility functions for SpeedCore wall assemblies. Damage state details are provided in Table 4.

3.2.2. SpeedCore Coupling Beam Fragilities

SpeedCore coupling beam fragilities were developed within a previous study conducted for AISC (Welch et al. 2024). The fragility development is based on experimental testing conducted at Purdue University. A total of six coupling beam specimens were used for fragility development. Coupling beam aspect ratios (L_{CB}/d_{CB}) varied from 3.5 to 5.1. A total of four different connection details were used for the tested specimens. A summary of the coupling beam test specimens is provided in Table 5.

Table 5. Experimental testing used for SpeedCore coupling beam fragility development (Welch et al. 2024)

References	Specimen[a]	Aspect Ratio L_{CB}/d_{CB}	Connection Type
Ahmad et al. (2020); Ahmad et al. (2024)	SP-1	3.5	1A – Beam web continuous with wall plate; beam flange plates wider than wall.
	SP-2	3.5	1B – Beam web separate plate from wall; interrupted wall flange plate.
	SP-3	5.1	1B – Beam web separate plate from wall; interrupted wall flange plate.
	SP-4	3.5	3 – Beam web continuous with wall plate; beam flanges equal the wall inside thickness.

SP-5	3.5	2 – Beam web separate plate from wall; continuous wall flange.
SP-6	5.1	2 – Beam web separate plate from wall; continuous wall flange.

[a] Specimen IDs are from Ahmad et al. (2020)

Fragility development used coupling beam rotation as an EDP. FEMA P-58-1 Appendix H (FEMA, 2018) was followed when developing the fragility functions. The fragility functions for SpeedCore coupling beams are comprised of three sequential damage states. DS1 represents the onset of visible damage and is split into two mutually exclusive DSs to either conduct or neglect minor repairs. DS2 is closely associated with displacement demands corresponding to peak strength, while DS3 is closely associated with significant strength loss (i.e., >20% strength loss from peak resistance).

The coupling beam fragilities have only one damage state that causes SCSD, i.e., DS3, which is assigned Safety Class 2 and allows 25% of the components to be damaged (see Table 2). Due to the reliance on coupling beams to provide energy dissipation and to realize coupled behavior between walls, Safety Class 2 is assigned to DS3. This reflects the impact on the global lateral strength of the structural system resulting from complete damage of the couplings beams. Conversely, DS2 is not assigned a Safety Class since the coupling beams have not lost appreciable strength and would still provide global coupling of the wall assemblies.

A summary of the SpeedCore coupling beam fragility functions and corresponding safety class assignments is provided in Table 6. Figure 3 shows example photographs of each damage state. A plot of the fragility functions is provided in Figure 4. Additional details of SpeedCore coupling beam fragility development can be found in Welch et al. (2024).

Table 6. SpeedCore coupling beam fragility damage states and corresponding safety classes.

Damage State[a]	Median (θ)[b]	β	Safety Class[c]	Damage Description	Repair Measures
DS1a (0.5)	1.13%	0.28	0	Yielding, initial buckling, onset of weld or plate damage possible. No repair conducted	No repairs conducted.
DS1b (0.5)	1.13%	0.28	0	Yielding, initial buckling, onset of weld or plate damage possible.	Access for inspection. Heat-straighten any significant buckling. Clean and repair any local weld or plate damage.

DS2	1.99%	0.41	0	Initial fracture propagation into flange/web, visible buckling. No significant strength loss.	Shoring and access for inspection. Replace buckled plate sections. Clean and repair weld and plate fracture areas. Remove and replace slab as needed.
DS3	3.45%	0.29	2	Significant strength loss, complete fracture of flange.	Shoring and access for inspection. Cut out severely buckled and fractured steel areas. Replace damaged concrete as needed. Replace broken or removed tie-bars. Heat straighten or replace buckled plate sections. Clean and repair weld and plate fracture areas. Remove and replace slab as needed.

[a] Mutually exclusive damage states (e.g., DSXa and DSXb) include the probability of occurrence in parentheses
[b] Fragility function is a lognormal distribution with median and standard deviation of θ and β, respectively. The EDP is coupling beam rotation.
[c] SC 1 = 50%, SC 2 = 25%, SC 3 = 10% allowable quantity of damaged components per direction across all stories; SC 0 does not result in SCSD.

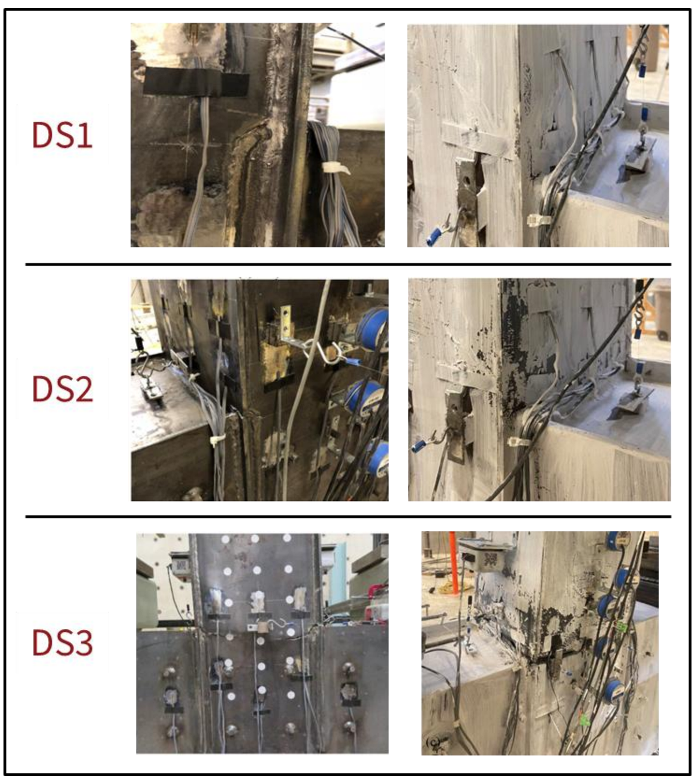

Figure 3. Examples of damage states for SpeedCore coupling beams (Welch et al. 2024).

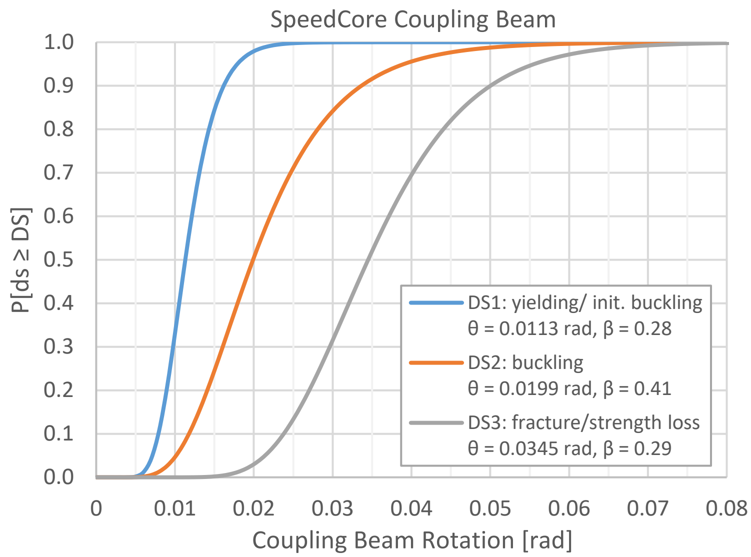

Figure 4. Fragility functions for SpeedCore coupling beams. Damage state details are provided in Table 6.

3.2.3. Steel Gravity Connection Fragilities

Steel gravity beam-to-column connections are based on fragility development by Deierlein and Victorsson (2008) during the FEMA P-58 Project and are available within the FEMA P-58 fragility database. The fragilities are based on thirteen experimental tests on simple bolted shear tab connections conducted by Liu and Astaneh (2000). Fragilities are developed using story drift ratio as the EDP.

Fragility functions for steel gravity connections are comprised of three sequential damage states with DS1 split into two mutually exclusive DSs to either conduct or neglect minor repairs. DS2 is assigned a Safety Class of 2, while DS3 is assigned a Safety Class of 3. The original FEMA P-58 fragilities assigned Safety Class 2 to both DS2 and DS3. Following review of the damage description for DS3, the Safety Class was increased to 3 to be more in line with the Safety Class definitions (see Table 2). A summary of the fragility functions and corresponding safety class assignments is provided in Table 7. Figure 5 shows example photographs of each damage state. A plot of the fragility functions is provided in Figure 6.

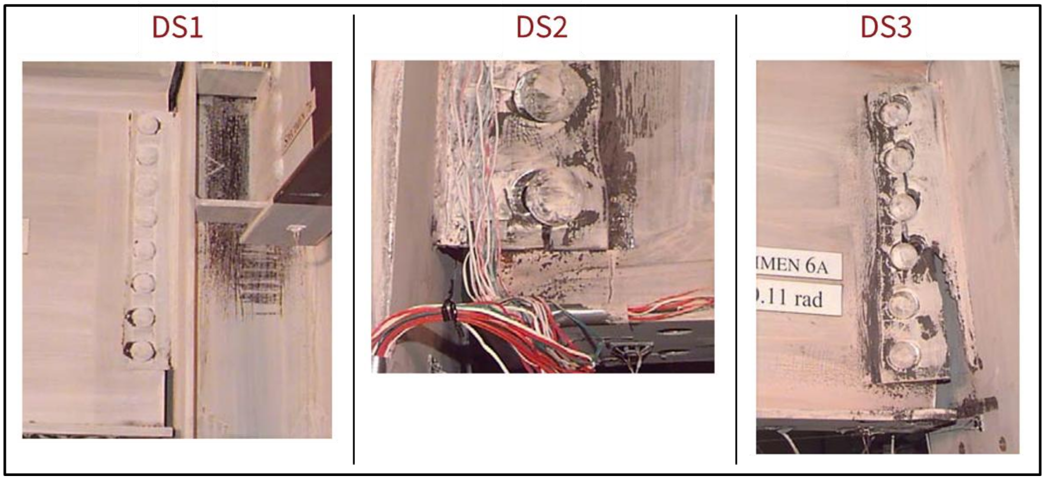

Figure 5. Damage states for bolted shear tab gravity connections (Deierlein and Victorsson, 2008).

Table 7. Bolted shear tab gravity connection fragility damage states and corresponding safety classes.

Damage State[a]	Median (θ)[b]	β	Safety Class[c]	Damage Description	Repair Measures
DS1a (0.95)	4.00%	0.4	0	Yielding of shear tab and elongation of bolt holes, possible crack initiation around bolt holes or at shear tab weld. Damage in field is either obscured or deemed to not warrant repair. No repair conducted.	Careful inspection and welded repair to any cracks and possible replacement of shear tab if bolt hole deformations are excessive (possible for deeper 6-bolt or deeper shear tabs). Field condition is deemed to not warrant repair by field observation.
DS1b (0.05)	4.00%	0.4	0	Yielding of shear tab and elongation of bolt holes, possible crack initiation around bolt holes or at shear tab weld.	Careful inspection and welded repair to any cracks and possible replacement of shear tab if bolt hole deformations are excessive (possible for 6-bolt or deeper shear tabs).
DS2	8.00%	0.4	2	Partial tearing of shear tab and possibility of bolt shear failure (6-bolt or deeper connections).	Repairs will include either welded repair of shear tab or possible complete replacement of shear tab and installation of new bolts. Repairs may require shoring of beam.
DS3	11.00%	0.4	3[d]	Complete separation of shear tab, close to complete loss of vertical load resistance.	Repair will include complete replacement of shear tab and installation of new bolts. Repairs will require shoring of beam.

[a] Mutually exclusive damage states (e.g., DSXa and DSXb) include the probability of occurrence in parentheses

[b] Fragility function is a lognormal distribution with median and standard deviation of θ and β, respectively. The EDP is story drift ratio.

[c] SC 1 = 50%, SC 2 = 25%, SC 3 = 10% allowable quantity of damaged components per direction per story; SC 0 does not result in SCSD.

[d] Original FEMA P-58 database assigns this damage state as Safety Class 2. This report deviates from the original FEMA P-58 database assignment by mapping to a more conservative safety class.

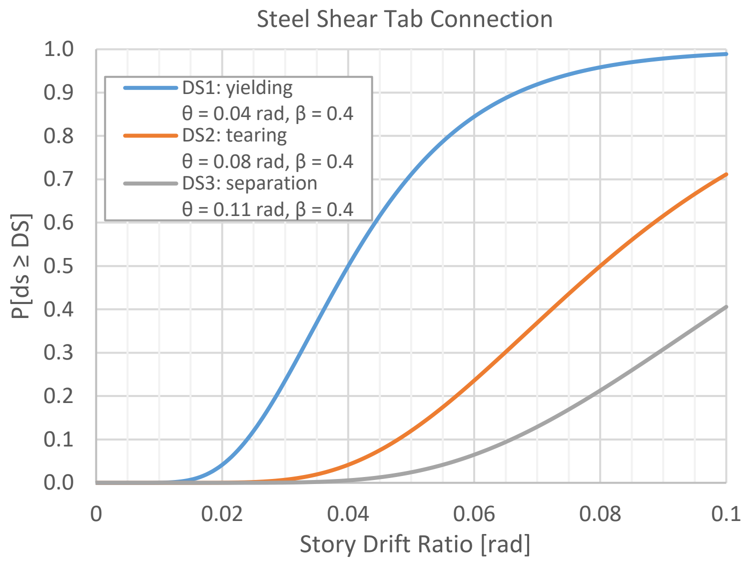

Figure 6. Fragility functions for bolted shear tab gravity connections. Damage state details are provided in Table 7.

3.3. Archetypes Considered for Analysis

To determine the combination of R_{fr} and Δ_{afr} that results in acceptable functional recovery performance, an archetype space is broken up into performance groups, analyzed, and the overall parameters are determined by the worst-case of the performance groups. This is similar to the FEMA P-695 methodology used for quantifying performance factors for life-safety (FEMA, 2009) and is in accordance with the proposed Section A.8 procedures of the 2026 NEHRP Provisions.

3.3.1. Building Configuration and Structural Component Population

All archetypes assume a constant plan area of 100 feet by 100 feet. Story heights are assumed to be 14 and 12 feet for the first and typical stories, respectively.

Uncoupled wall systems assume that there are two planar (rectangular) walls in each principal direction in plan. Coupled wall systems 15 stories and above assume a symmetrical core that is comprised of two coupled walls and one coupling beam on each side in plan, totaling 4 wall assemblies and 2 coupling beams for each principal direction. Coupled wall systems below 15 stories have the same number of wall and coupling beam assemblies, but the walls are planar and not in a core configuration. Steel gravity connections are populated based on an assumed 25-foot bay gravity frame spacing, accounting for the locations of the walls. An illustration of the plan layout and populated structural components for both uncoupled and coupled SpeedCore systems is provided in Figure 7.

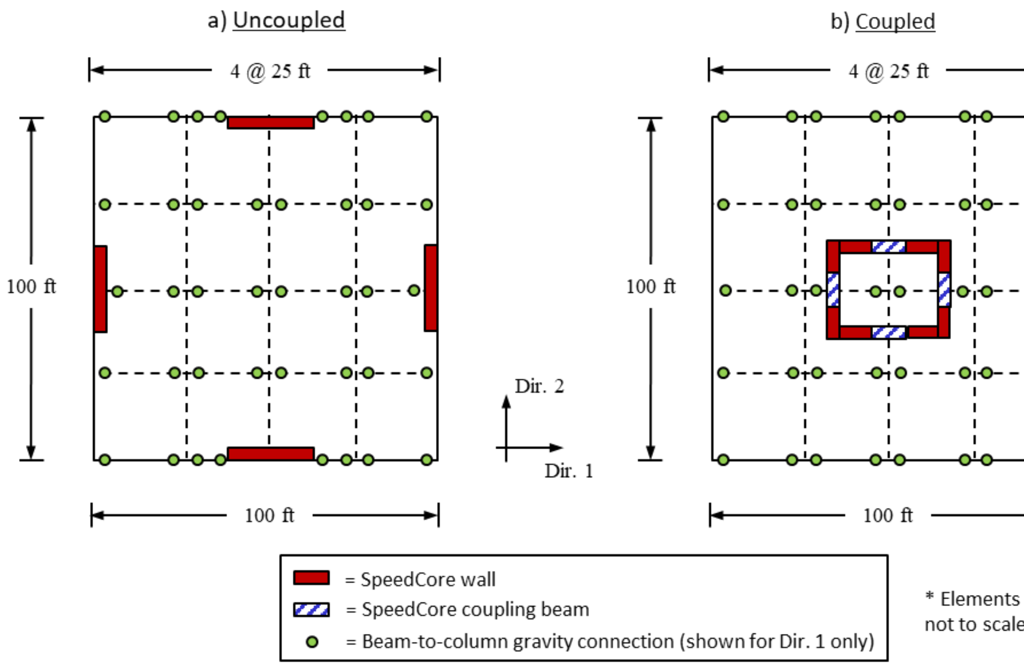

Figure 7. Illustration of assumed plan layout and structural component population for SpeedCore archetypes: a) uncoupled, b) coupled 15 stories and above.

3.3.2. Performance Groups for SpeedCore Wall Systems

The performance groups considered for the uncoupled variant were low, mid, and high-rise buildings of the heights used in determining seismic performance factors for life-safety using the FEMA P-695 analysis for the uncoupled SpeedCore system (Agrawal et al. 2020; Broberg et al. 2023; Kizilarslan and Bruneau, 2023b). The number of stories in each performance group are shown in Table 8. The sensitivity to the gravity system was also investigated by running a rugged gravity frame variant in addition to the steel frame gravity system variant.

Table 8. SpeedCore performance group summary of building heights.

Performance Group	Uncoupled No. Stories	Coupled No. Stories
PG1 (low-rise)	3, 6	4, 6
PG2 (mid-rise)	8, 10, 12	8, 10, 12
PG3 (high-rise)	15, 18	15, 18

The performance groups considered for the coupled variant were low-rise, mid-rise, and high-rise buildings of the heights used in determining seismic performance factors for life-safety using the FEMA P-695 analysis for the coupled SpeedCore system (Bruneau et al. 2019; Kizilarslan et al. 2021b). For both coupled and uncoupled walls, the story heights were assumed to be 14ft for the first story and 12ft for the upper stories. This was selected as a reasonable middle ground between the heights of 17/14ft (SpeedCore) and the 10/10ft (RCSW) P-695 archetypes. One exception was made for the 4-story coupled variant; all stories were assumed to be 15ft to meet the 60ft minimum height requirement (per footnote *q* of ASCE 7-22 Table 12.2-1).

An important aspect of P[SCSD] for coupled walls is the coupling beam rotation. This parameter is highly dependent on the relative length of the coupling beam, L_{cb}, and the distance between wall centroids, L_{wc} as discussed in Section 3.4.5. The coupling beam amplification ratio (CBAR), L_{wc}/L_{cb}, is the primary coupling beam related geometric parameter that is varied in the archetypes. To simplify this variation, four lengths of coupling beams were chosen: 6ft, 7ft-6in, 8ft-4in, and 12ft. With the coupling beam aspect ratios limited to the range of 3 to 5 (length of the coupling beam to the depth of the coupling beam), these coupling beam lengths are reasonable to pair with coupling beam depths in the range of 24-30in. The wall lengths were varied to capture the expected range of the CBAR. To capture the extremes of the expected range, the longest coupling beams were coupled with shorter walls creating a low CBAR and vise versa.

The expected ranges of the CBAR were selected using the envelope of ratios from the SpeedCore P-695 study (Kizilarslan and Bruneau, 2023b) as well as the coupled RCSW P-695 study (Tauberg et al. 2019). The coupling beam lengths are comparable between the two studies, but the floorplan of the SpeedCore archetypes is 120ft by 200ft (24,000 SF) as opposed to the RCSW study which has a floorplan of 102ft by 102ft (10,404 SF). Due to the higher seismic mass, the length of walls in the SpeedCore archetypes are notably greater than the RCSW variants, causing the higher CBAR shown in Figure 8. Since both floorplans are reasonable, the CBAR range from both studies are considered together for this study.

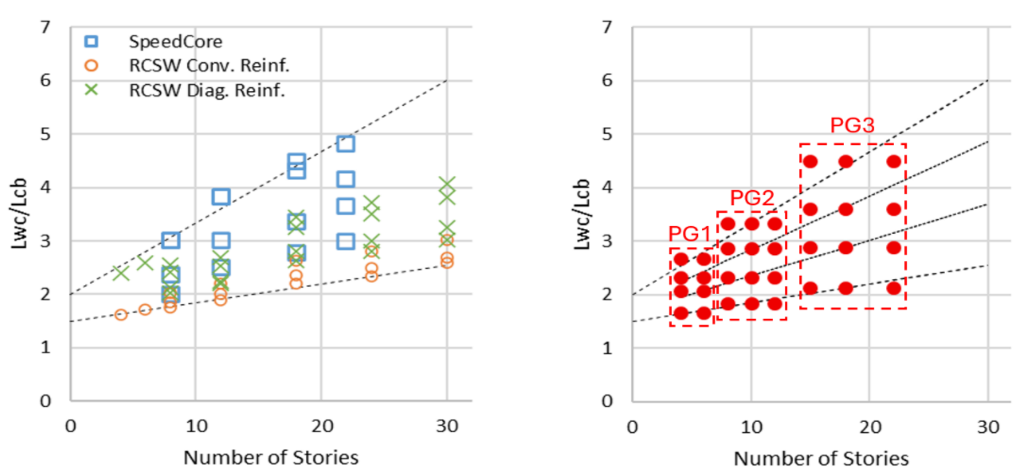

Figure 8: Range of coupling beam amplification ratio (CBAR) for the SpeedCore and RCSW P-695 study archetypes: Individual archetype designs (left), Grouping assumed for each performance group (right).

The assumed wall and coupling beam geometries are summarized in Table 9. For planar walls, the dimension L_w is the length of the wall which results in the centroid of the wall being $0.5L_w$ from the end of the coupling beam. For the "L" shaped walls, both legs are assumed to have the same length which results in the centroid of the wall being approximately $0.75L_w$ from the end of the coupling beam.

Table 9: Coupling beam and wall length combinations assumed for the coupled performance groups.

		L_{cb} = 12' 0"		L_{cb} = 8' 4"		L_{cb} = 7' 6"		L_{cb} = 6' 0"	
PG	**Wall Shape**	**L_w (ft)**	**CBAR**	**L_w (ft)**	**CBAR**	**L_w (ft)**	**CBAR**	**L_w (ft)**	**CBAR**
PG1	Planar	8	**1.67**	9	**2.08**	10	**2.33**	10	**2.67**
PG2	Planar	10	**1.83**	11	**2.32**	14	**2.87**	14	**3.33**
PG3	"L"	9	**2.13**	10.5	**2.89**	13	**3.6**	14	**4.5**

3.4. Estimation of Structural Responses

The structural responses for the archetypes were determined using the SP3 Structural Response Prediction Engine (SRPE). The SRPE generates a simplified linear multi-degree-of-freedom model representative of strength and stiffness requirements outlined by Miranda (Miranda, 1999; Miranda and Reyes, 2002). Nonlinear response is determined by sampling from Incremental Dynamic Analysis (IDA: Vamvatsikos and Cornell, 2002) results from high-fidelity nonlinear models with similar linear characteristics. Further details on this methodology are documented in Cook et al. (2018) and by HB-Risk (Haselton Baker Risk Group, 2025).

The structural responses for the archetypes were obtained from the SpeedCore Structural Response Prediction Engine (SRPE) developed previously for AISC (Almeter et al. 2024). This sub-section provides an overview of the analytical basis behind the SRPE as well as the quantification of different Engineering Demand Parameters (EDPs). More detailed information can be found in Almeter et al. (2024).

3.4.1. Analytical Basis Behind the SpeedCore Structural Response Prediction Engine (SRPE)

The SpeedCore SRPE is based on calibration to 23 different buildings modeled in OpenSees (McKenna et al. 2010). The models were provided by the same analysts that conducted the FEMA P-695 (FEMA, 2009) assessments to develop the building seismic performance factors (e.g., R) for life-safety in uncoupled (Agrawal et al. 2020; Broberg et al. 2023; Kizilarslan and Bruneau, 2023b) and coupled (Bruneau et al. 2019; Kizilarslan et al. 2021b) SpeedCore systems. A summary of the different archetype buildings considered for SRPE calibration is provided in Table 10. The models consist of 16 coupled and 7 cantilever (i.e., uncoupled) wall buildings.

Buildings up to 12 stories are designed as planar walls and taller models are designed as C-shaped walls. Coupled wall variants have a constant coupling beam depth of 24 inches and 18 inches for D_{max} and D_{min} archetypes, respectively.

All models were analyzed using the FEMA P-695 far-field ground motion set (FEMA, 2009) consisting of 44 ground motions (i.e., 22 horizontal pairs). Incremental Dynamic Analysis (IDA: Vamvatsikos and Cornell, 2002) was used to obtain a range of linear and nonlinear structural responses for calibration.

The key EDPs for structural response prediction of the SpeedCore system are story drift ratio, wall chord rotation, and coupling beam rotation (as applicable). The SpeedCore SRPE distinguishes between coupled and uncoupled wall systems, reflecting the different sources of nonlinearity inherent to each system type. An overview of the estimation of these EDPs are discussed in the following sub-sections.

Table 10. Summary of building models used for calibration of the SpeedCore SRPE (Almeter et al. 2024).

Model ID	Stories	Configuration	Properties Reference
PG-1A	8	Planar, Coupled, 6ft Coupling Beam, D_{max}	Kizilarslan et. al (2021b)
PG-1B	8	Planar, Coupled, 8ft Coupling Beam, D_{max}	Kizilarslan et. al (2021b)
PG-1C	8	Planar, Coupled, 10ft Coupling Beam, D_{max}	Kizilarslan et. al (2021b)
PG-2B	8	Planar, Coupled, 6ft Coupling Beam, D_{min}	Kizilarslan et. al (2021b)
PG-1D	12	Planar, Coupled, 6ft Coupling Beam, D_{max}	Kizilarslan et. al (2021b)
PG-1E	12	Planar, Coupled, 8ft Coupling Beam, D_{max}	Kizilarslan et. al (2021b)
PG-1F	12	Planar, Coupled, 10ft Coupling Beam, D_{max}	Kizilarslan et. al (2021b)
PG-2E	12	Planar, Coupled, 6ft Coupling Beam, D_{min}	Kizilarslan et. al (2021b)
PG-3A	18	C-shaped, Coupled, 6ft Coupling Beam, D_{max}	Kizilarslan et. al (2021b)
PG-3B	18	C-shaped, Coupled, 8ft Coupling Beam, D_{max}	Kizilarslan et. al (2021b)
PG-3C	18	C-shaped, Coupled, 10ft Coupling Beam, D_{max}	Kizilarslan et. al (2021b)
PG-4B	18	C-shaped, Coupled, 6ft Coupling Beam, D_{min}	Kizilarslan et. al (2021b)
PG-3D	22	C-shaped, Coupled, 6ft Coupling Beam, D_{max}	Kizilarslan et. al (2021b)
PG-3E	22	C-shaped, Coupled, 8ft Coupling Beam, D_{max}	Kizilarslan et. al (2021b)
PG-3F	22	C-shaped, Coupled, 10ft Coupling Beam, D_{max}	Kizilarslan et. al (2021b)
PG-4E	22	C-shaped, Coupled, 6ft Coupling Beam, D_{min}	Kizilarslan et. al (2021b)
3-S1	3	Planar, Cantilever, D_{max}	Broberg (2023)
6-S1	6	Planar, Cantilever, D_{max}	Broberg (2023)
9-S1	9	Planar, Cantilever, D_{max}	Broberg (2023)
12-S1	12	Planar, Cantilever, D_{max}	Broberg (2023)
15-S1	15	C-shaped, Cantilever, D_{max}	Broberg (2023)
18-S1	18	C-shaped, Cantilever, D_{max}	Broberg (2023)
22-S1	22	C-shaped, Cantilever, D_{max}	Broberg (2023)

3.4.2. Structural Properties Estimation

Building structural properties are estimated using a linear building model, with strength and stiffness scaled to meet corresponding design requirements. Typical levels of overstrength (e.g., due to expected material properties, etc.) are added after design requirements are satisfied, to provide the best possible estimate of the true strength and stiffness of the LFRS. The commercial version of SP3 also includes additional strength and stiffness contributions from the gravity system and nonstructural components, but these are excluded in this study for compliance with the procedures of section A.8 of the 2026 National Earthquake Hazards Reduction Program (NEHRP) Provisions.

The process begins by determining the design parameters, including spectral values, response modification factor (R), deflection amplification factor (C_d), and related values (e.g., I_e). Next, a target seismic design drift is selected. For drift-controlled systems, such as most moment frames, this target is typically the design drift limit—for example, 2% for risk category II buildings. For strength-controlled systems, the target drift is a realistic value appropriate for the system type and building height; the expected design drift values are based on a database of hundreds of building designs (from archetype buildings in the SP3 SRPE database). Resilient design iterations use the same process with pairs of R_{fr} and Δ_{afr} for a given analysis. Notably, the deflection amplification factor (C_d) is taken equal to R_{fr} and the building importance factor (I_e) is taken as unity per Section A.8 of the 2026 NEHRP Provisions.

Following this, the period of a representative design model (limited to the lateral force-resisting system, or LFRS) is determined, considering the target seismic drift and stability requirements (ASCE 7-22 Section 12.8.7). This involves constructing a simple multi-degree-of-freedom (MDOF) model that reflects the system's mass and stiffness characteristics. For instance, moment frames tend to be more shear-dominated, whereas walls and braced frames are more flexure-dominated. This approach is based on a method developed by Miranda (1999) and Miranda and Reyes (2002) but utilizes matrix structural analysis—with mass and stiffness matrices—rather than purely analytical equations; it also incorporates the ability to model rotational flexibility at the base.

Starting with very low stiffness, the stiffness matrix is systematically scaled (i.e., increased) until the model achieves the target drift or less, while also satisfying stability requirements. Generally, modal response spectrum analysis (MRSA) is used to generate structural properties for buildings that are modern code-compliant, taller than four stories, and located in high or very high seismic areas. For other cases, the equivalent lateral force (ELF) procedure is used. Wind drift checks can be included in this step but were omitted for this study.

Next, the expected strength and stiffness of the LFRS are determined, accounting for overstrength. These properties vary depending on the LFRS type and building height and are calibrated using results from OpenSees models and engineering judgment. An additional optional check can be performed to ensure compatibility between strength and stiffness. If the stiffness is found to be too low in relation to the strength and yield drift, it is increased to a reasonable level. Archetypes for this study are developed with and without including the optional strength/stiffness compatibility check.

The final estimates of the first three periods and mode shapes of the building are determined by performing an eigen analysis with the stiffness matrix and mass matrix. The final estimate of the ultimate base shear strength is determined from design strength and the expected overstrength.

3.4.3. Story Drift Ratio

The SpeedCore SRPE estimates median story drift ratio by first estimating linear response at the intensity of interest, then adjusting for nonlinear demands. Linear response is estimated from the first three modes of the building. Nonlinear demands are adjusted based on the intensity factor S = $S_a/(V_{max}/W)$, where S_a is the first mode spectral acceleration of interest and (V_{max}/W) represents the normalized peak strength of the building using expected properties. Nonlinear adjustment is based on the intensity (i.e., S value), height of the building (i.e., number of stories), and location in elevation (i.e., story number). Nonlinear adjustments differ for coupled and uncoupled wall systems. An example calibration for an 8-story building model is shown in Figure 9. The dashed lines represent the median drift profile from nonlinear response history analysis (NRHA) compared to SRPE response shown in solid lines. The dotted lines show the linear response prediction before adjusting for nonlinear behavior.

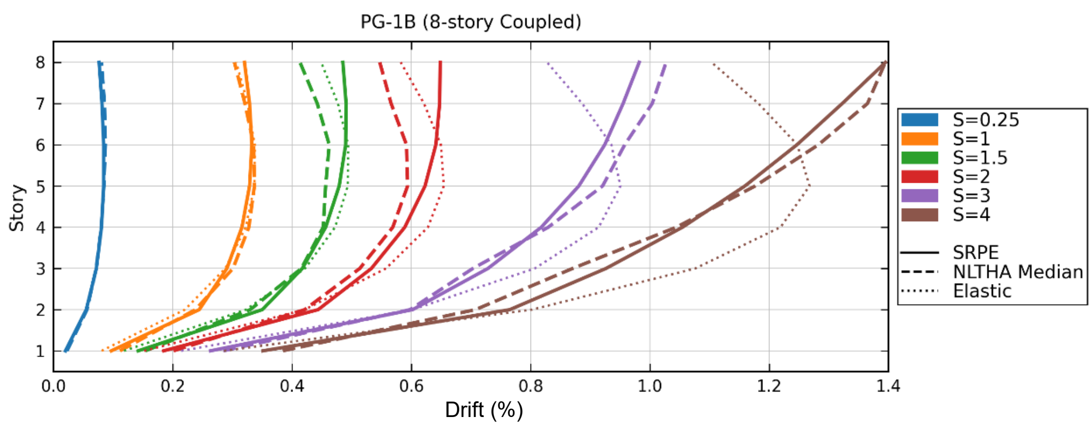

Figure 9. Comparison of SRPE (solid) and median NRHA (dashed) story drift ratio response for model PG-1B. Note dotted lines represent predicted linear response scales to the expected roof displacement prior to adjustment for nonlinear behavior. The various "S" values are different levels of inelasticity ($S=Sa(T_1)/v_{ult}$). Figure adapted from Almeter et al. (2024).

3.4.4. Wall Chord Rotation

The chord rotation at the base of the wall is estimated by converting the SRPE story drift profile to a global displaced shape. There is an adjustment factor to convert the peak story drift profile to a peak transient drift profile since the peak drift does not occur simultaneously at each level, especially for taller buildings. The global rotation at the first mode effective height is taken as the total chord rotation demand at the wall base. An illustration of this calculation is shown in Figure 10, where θ_{wall} represents the wall chord rotation at the base. This approximation of wall chord rotation targets consistency with the development of fragility functions (see Section 3.2) while relying on the story drift calibration to adequately capture differences in building height as well as coupled versus uncoupled behavior.

The chord rotation demand at upper stories is not as critical for estimating wall damage; these values are numerically calibrated to nonlinear models as ratios of the base chord rotation. The chord rotation at upper levels tends to be nearly an order of magnitude lower than the base chord rotation. An example response calibration plot is shown in Figure 11.

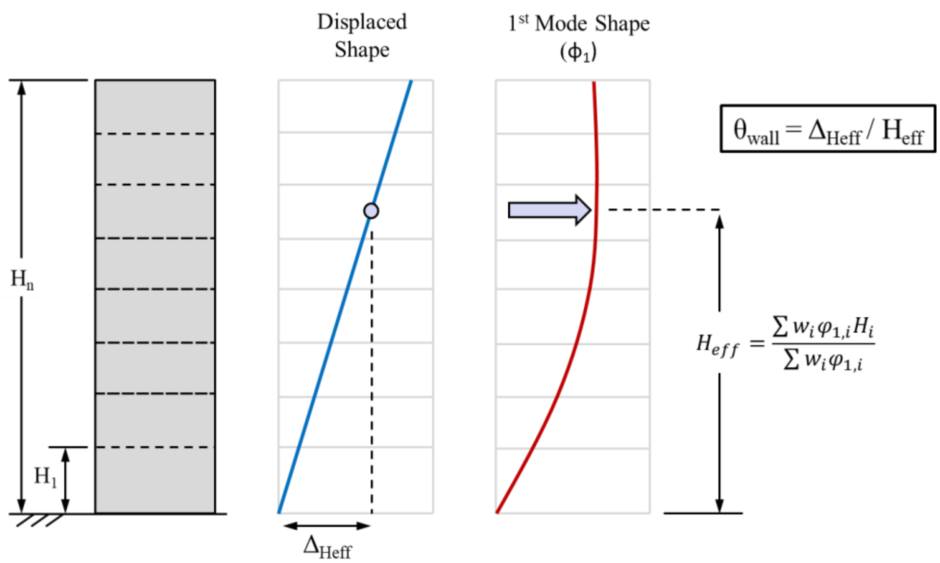

Figure 10. Illustration of using the displacement at the first mode effective height to approximate the total chord rotation at the base of SpeedCore walls.

Chord Rotation (%)

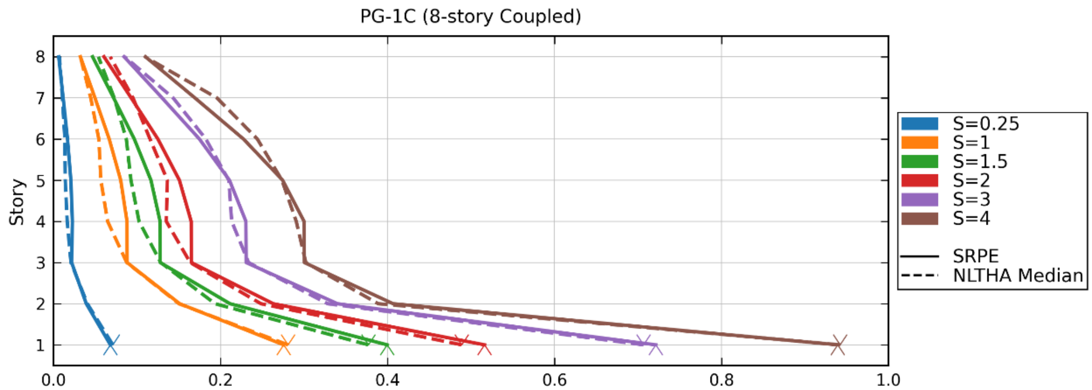

Figure 11: Comparison of SRPE (solid) and median NRHA (dashed) peak chord rotation response for an 8-story Coupled SpeedCore wall. The various "S" values are different levels of inelasticity ($S=Sa(T_1)/v_{ult}$). Figure adapted from Almeter et al. (2024).

3.4.5. Coupling Beam Rotation

Coupling beam rotation response is estimated based on the story drift demand (θ_{drift}), coupling beam length (L_{cb}), wall centroid distance (L_{wc}), as well as the effects of the axial deformation in the walls (θ_{floor}). The relationship between drift and coupling beam rotation (White and Adebar, 2004) is expressed as:

$$\theta_{cb} = \left(\theta_{drift} - \theta_{floor}\right)\frac{L_{wc}}{L_{cb}}$$

where

θ_{cb}	coupling beam rotation
θ_{drift}	story drift
θ_{floor}	rotation of the floor from axial shortening/elongation of the walls
L_{wc}	distance between the centroids of the walls
L_{cb}	clear span length of the coupling beam

The counter-acting effects of story drift and wall axial elongation are shown in Figure 12. The NRHA results showed that the peak coupling beam rotation at each level tended to occur at the peak story drift, so the SP3 SRPE for drift is used without modification to predict the θ_{drift} value at each level. The parameter θ_{floor} was calibrated to the NRHA such that when combined with the other parameters (θ_{drift} , L_{cb}, and L_{wc}), a proper estimate of coupling beam rotation, θ_{cb}, was achieved.

Example calibrations of the coupling beam rotations are shown in Figure 13. Note that the coupling beam rotations increase for the higher CBAR case. The dashed lines represent the median drift profile from nonlinear response history analysis (NRHA) compared to SRPE response shown in solid lines.

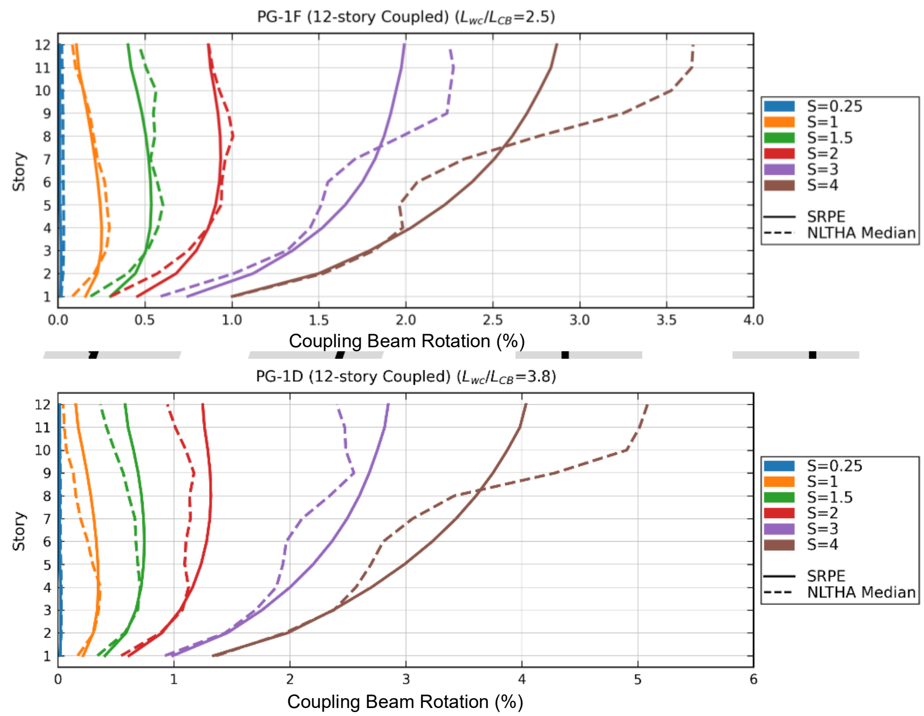

Figure 12: Coupling beam ratio calibrations for 12-story Coupled SpeedCore walls with CBAR values of 2.5 (top) and 3.8 (bottom). Note that the axis scales are different for the two cases.

3.4.6. Peak Floor Acceleration

Peak floor acceleration (PFA) is computed based on spectral acceleration, building strength, and the first three modal periods and shapes of the building. First, elastic PFA is computed with modal time-history analysis using the FEMA P-695 far-field record set scaled to the intensity of interest. Then, if the spectral acceleration demand is large enough to cause yielding, PFA is adjusted using the intensity factor $S = S_a/(V_{max}/W)$. The amount of reduction of the response depends on how high the story is above the ground, because damage in the lower stories "isolates" the upper stories from acceleration input.

An example calibration for an 8-story Coupled SpeedCore wall is shown in Figure 14. The dashed lines represent the median PFA profile from NRHA compared to SRPE response shown in solid lines. The dotted lines show the elastic response profile before adjusting for nonlinear behavior. Note that the largest intensity shaking (brown lines) has significant reductions from the elastic prediction at upper stories due to damage in the lower stories.

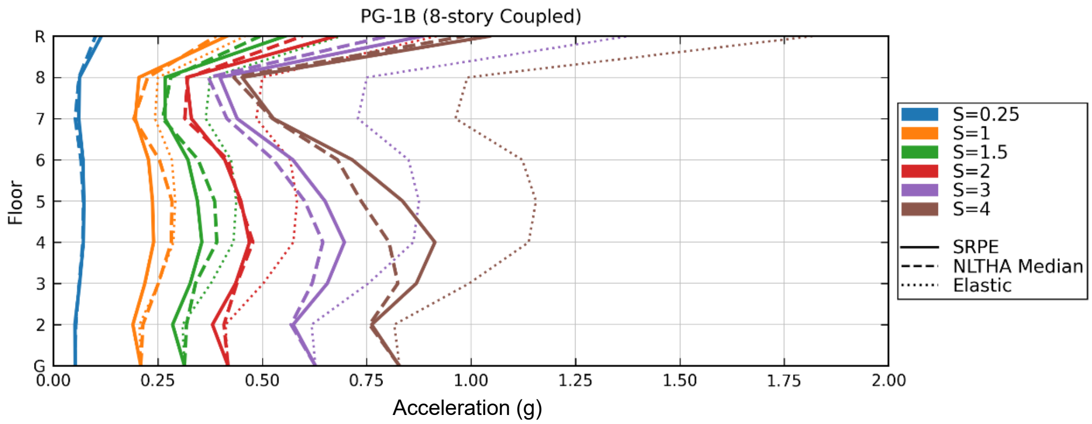

Figure 14. Comparison of SRPE (solid) and median NRHA (dashed) peak floor acceleration response for an 8-story Coupled SpeedCore wall. Note, dotted lines represent predicted linear response prior to adjustment for nonlinear behavior. The various "S" values are different levels of inelasticity ($S=Sa(T_1)/v_{ult}$). Figure adapted from Almeter et al. (2024).

3.4.7. Residual Drift Ratio

The FEMA P-58 residual drift modeling was updated during the ATC-138 project (ATC, 2021) and resulted in a supplemental FEMA P-58 background document *BD 3.7.26: Updated Model and Criteria for Residual Drift* (DeBock et al. 2024). The revisions to the original FEMA P-58 model allowed for distinctions between structural systems, based on recent analytical studies (Almeter et al. 2018; Vouvakis Manousakis et al. 2024).

The median residual story drift ratio (Δ_r) is estimated from the median transient story drift ratio (Δ) and yield drift ratio (Δ_y). The general format for simplified residual drift estimation has a trilinear form with a transition slope and a primary slope. The initial slope represents the elastic response range (i.e., $\Delta \leq \Delta_y$) where residual displacement is not expected. The transition slope reduces the rate of residual drift accumulation in the region just beyond elastic response to a specified drift ductility, after which, the steeper primary slope accumulates residual drift at a faster rate as peak drift demands increase. The end of the transition region is defined by a system specific drift value Δ_{shift}. An illustration of the basic components of the trilinear residual drift model is shown in Figure 15.

Three residual drift models were developed as part of the FEMA P-58 revisions, with parameters summarized in Table 11. For the SpeedCore system, the RC Wall model is selected according to the FEMA P-58 recommendations, listed in Table 12. The recommended yield drift ratio (Δ_y) of 0.25% is also taken from Table 12. The residual story drift ratio as a function of story drift ratio demand for the Steel SMF system is shown in Figure 16.

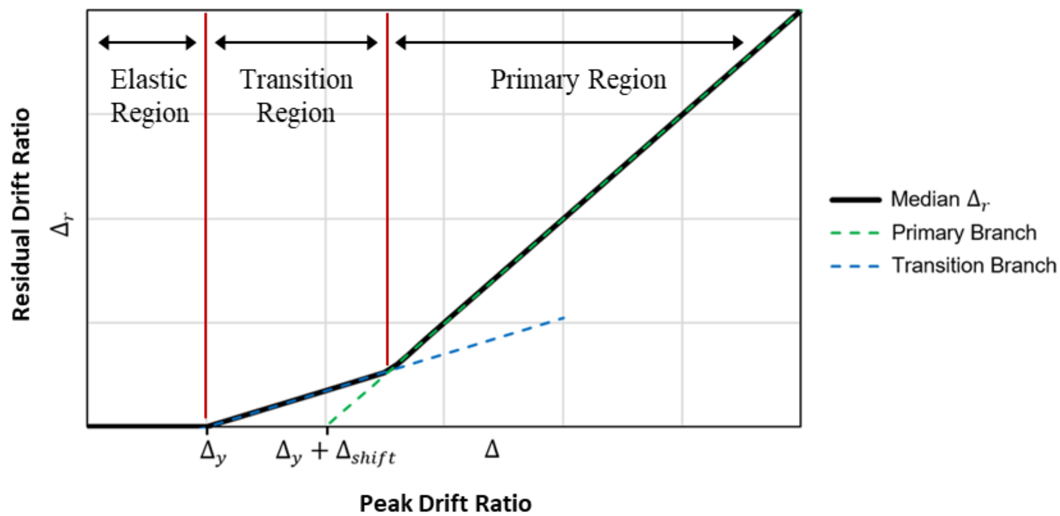

Figure 15 – Basic components of the trilinear model to estimate residual story drift as a function of peak story drift demand and yield story drift.

Table 11. Parameters of updated FEMA P-58 residual drift models

Residual Drift Model	**Δ_{shift}**	**Primary Slope (a)**	**Transition Slope (b)**
Steel MRF	0.005	0.5	0.2
BRBF	0.007	0.4	0.1
General Inelastic	0.008	0.35	0.15

Table 12. Recommended yield story drift ratio (Δ_y) and residual drift models by LFRS

LFRS	**Δ_y (rad)**	**Residual Drift Model**
Steel MRF	0.01	Steel MRF
Steel CBF	0.003	General Inelastic
Steel EBF	0.005	BRBF
Steel BRBF	0.002	BRBF
RC MF	0.0075	General Inelastic
RC Wall	0.0025	General Inelastic
Masonry	0.0025	General Inelastic
Wood or CFS light frame	0.075	General Inelastic

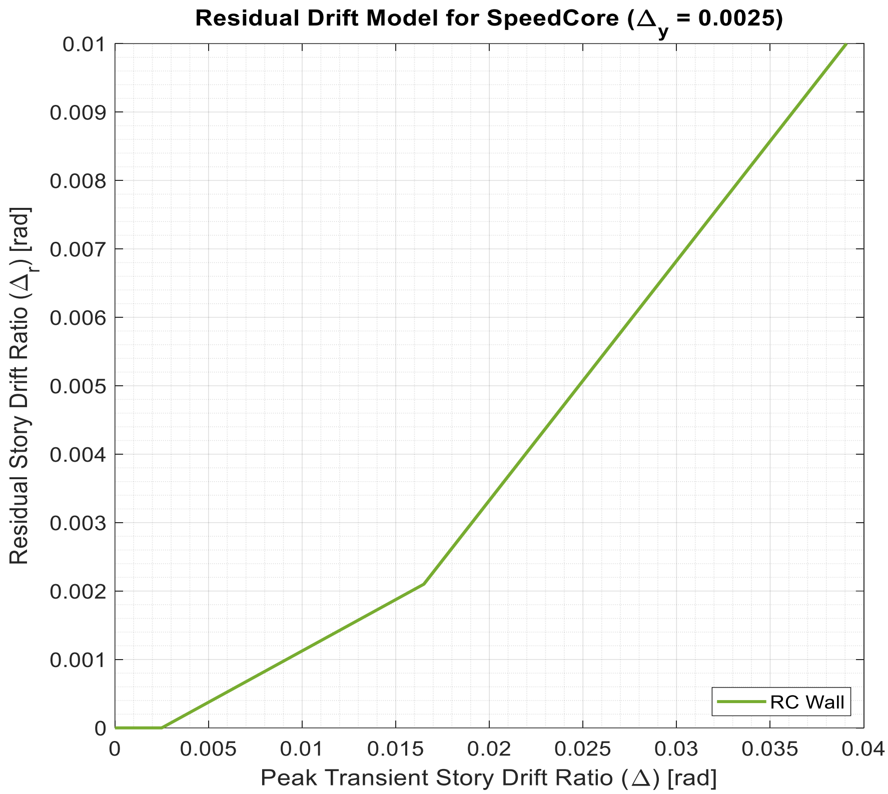

Figure 16. Residual drift model for the SpeedCore structural system

4. RESULTS

The tables and plots below show the R_{fr} and Δ_{afr} envelope for the for each performance group variant combination. This design envelope identifies the possible design value combinations where all performance groups satisfy both the max and mean analysis criteria. Results are provided separately for both FRC A/B/C acceptance criteria in Section 4.1 and FRC D acceptance criteria in Section 4.2. Additional figures are provided that illustrate general system performance in terms of structural response, controlling component damage and controlling design features are provided in Section 4.3. Full details on the performance of individual archetypes are provided in the attached supplementary materials.

4.1. FRC A/B/C Analysis Results

Table 13 – R_{fr} values across various allowable drift limits required to satisfy the FRC A/B/C structural performance acceptance criteria for each performance group.

	Δ_{afr}							
Performance Group [1, 2, 3, 4]	0.005	0.0075	0.01	0.0125	0.015	0.0175	0.02	Criteria
PG1-SC-UC-R	6.5	6.5	6.5	6.5	6.5	6.5	6.5	Max
PG1-SC-UC-SF	6.5	6.5	6.5	6.5	6.5	6.5	6.5	
PG2-SC-UC-R	6.5	6.5	6.5	6.5	6.5	6.5	6.5	
PG2-SC-UC-SF	6.5	6.5	6.5	6.5	6.5	6.5	6.5	
PG3-SC-UC-R	6.5	6.5	6.5	6.5	6.5	6.5	6.5	
PG3-SC-UC-SF	6.5	6.5	6.5	6.5	6.5	6.5	6.5	
PG1-SC-C-R	8	8	6.5	6	6	6	6	
PG1-SC-C-SF	8	8	6.5	6	6	6	6	
PG2-SC-C-R	8	6.5	3.5	3	3	3	3	
PG2-SC-C-SF	8	6.5	3.5	3	3	3	3	
PG3-SC-C-R	8	8	3.5	3.5	3.5	3.5	3.5	
PG3-SC-C-SF	8	8	3.5	3.5	3.5	3.5	3.5	
PG1-SC-UC-R	6.5	6.5	6.5	6.5	6.5	6.5	6.5	Mean
PG1-SC-UC-SF	6.5	6.5	6.5	6.5	6.5	6.5	6.5	
PG2-SC-UC-R	6.5	6.5	6.5	6.5	6.5	6.5	6.5	
PG2-SC-UC-SF	6.5	6.5	6.5	6.5	6.5	6.5	6.5	
PG3-SC-UC-R	6.5	6.5	6.5	4.5	4.5	4.5	4.5	
PG3-SC-UC-SF	6.5	6.5	6.5	4.5	4.5	4.5	4.5	
PG1-SC-C-R	8	8	6.5	6	6	6	6	
PG1-SC-C-SF	8	8	6.5	6	6	6	6	
PG2-SC-C-R	8	6	3.5	3.5	3.5	3.5	3.5	
PG2-SC-C-SF	8	6	3.5	3.5	3.5	3.5	3.5	
PG3-SC-C-R	8	8	3.5	3.5	3.5	3.5	3.5	
PG3-SC-C-SF	8	8	3.5	3.5	3.5	3.5	3.5	

[1] UC – Uncoupled walls

[2] C – Coupled walls

[3] SF – Steel framing and connections gravity system

[4] R – "Rugged" gravity system

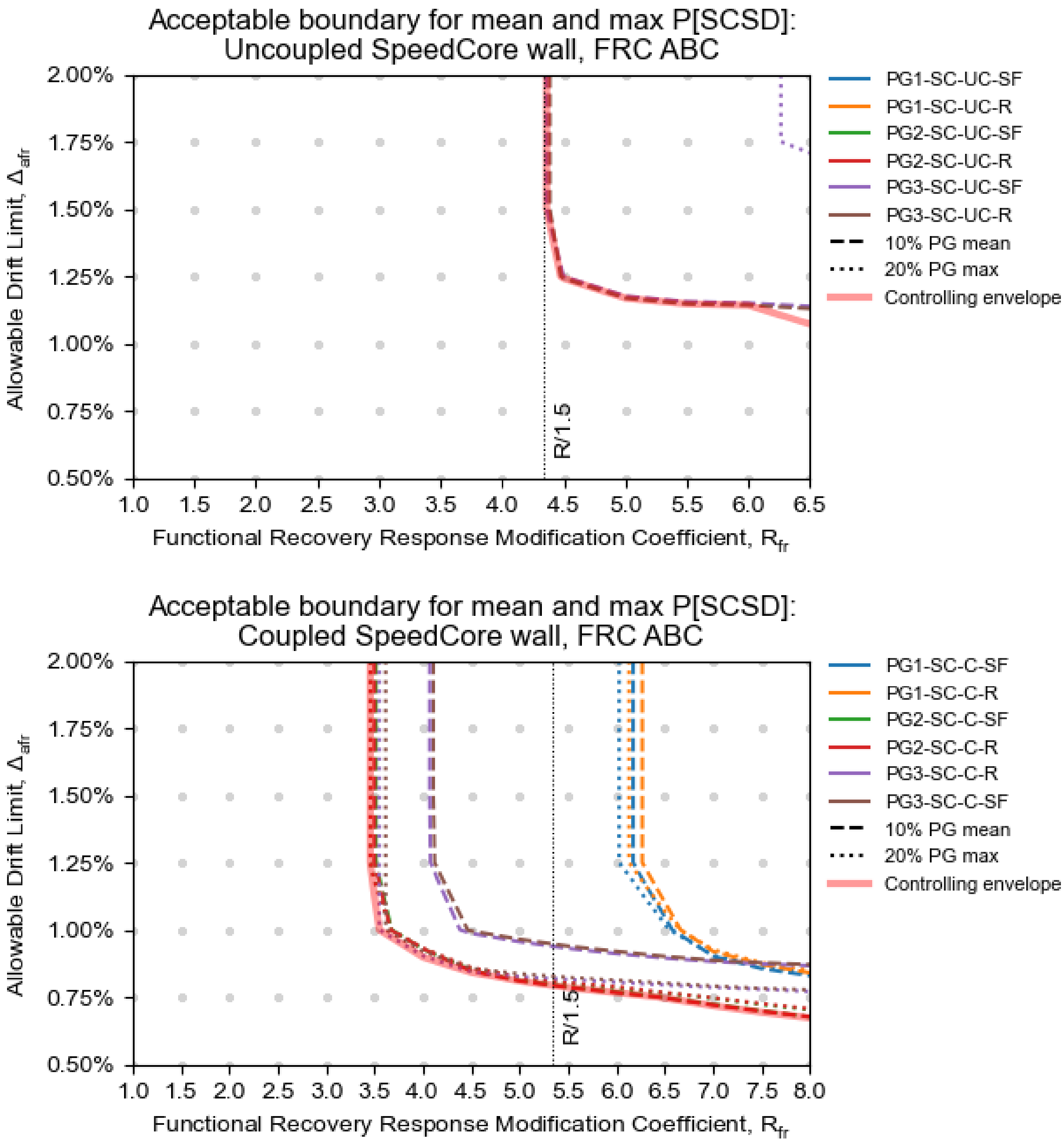

Figure 17 – Combination of R_{fr} and Δ_{afr} values required to satisfy the FRC A/B/C structural performance acceptance criteria for each performance group.

4.2. FRC D Analysis Results

Table 14 – R_{fr} values across various allowable drift limits required to satisfy the FRC D structural performance acceptance criteria for each performance group.

	Δ_{afr}							
Performance Group	0.005	0.0075	0.01	0.0125	0.015	0.0175	0.02	Criteria
PG1-SC-UC-R	6.5	6.5	6.5	6.5	6.5	6.5	6.5	Max
PG1-SC-UC-SF	6.5	6.5	6.5	6.5	6.5	6.5	6.5	
PG2-SC-UC-R	6.5	6.5	6.5	6.5	6.5	6.5	6.5	
PG2-SC-UC-SF	6.5	6.5	6.5	6.5	6.5	6.5	6.5	
PG3-SC-UC-R	6.5	6.5	6.5	6.5	6.5	6.5	6.5	
PG3-SC-UC-SF	6.5	6.5	6.5	6.5	6.5	6.5	6.5	
PG1-SC-C-R	8	8	7	6.5	6.5	6.5	6.5	
PG1-SC-C-SF	8	8	6.5	6	6	6	6	
PG2-SC-C-R	8	8	4	3.5	3.5	3.5	3.5	
PG2-SC-C-SF	8	8	4	3.5	3.5	3.5	3.5	
PG3-SC-C-R	8	8	3.5	3.5	3.5	3.5	3.5	
PG3-SC-C-SF	8	8	4	4	4	4	4	
PG1-SC-UC-R	6.5	6.5	6.5	6.5	6.5	6.5	6.5	Mean
PG1-SC-UC-SF	6.5	6.5	6.5	6.5	6.5	6.5	6.5	
PG2-SC-UC-R	6.5	6.5	6.5	6.5	6.5	6.5	6.5	
PG2-SC-UC-SF	6.5	6.5	6.5	6.5	6.5	6.5	6.5	
PG3-SC-UC-R	6.5	6.5	6.5	6.5	6	6	6	
PG3-SC-UC-SF	6.5	6.5	6.5	6.5	6.5	6.5	6.5	
PG1-SC-C-R	8	8	7.5	7	7	7	7	
PG1-SC-C-SF	8	8	7	7	7	7	7	
PG2-SC-C-R	8	8	4	4	4	4	4	
PG2-SC-C-SF	8	8	4	4	4	4	4	
PG3-SC-C-R	8	8	5	4	4	4	4	
PG3-SC-C-SF	8	8	5	4.5	4.5	4.5	4.5	

[1] UC – Uncoupled walls

[2]C – Coupled walls

[3]SF – Steel framing and connections gravity system

[4]R – “Rugged” gravity system

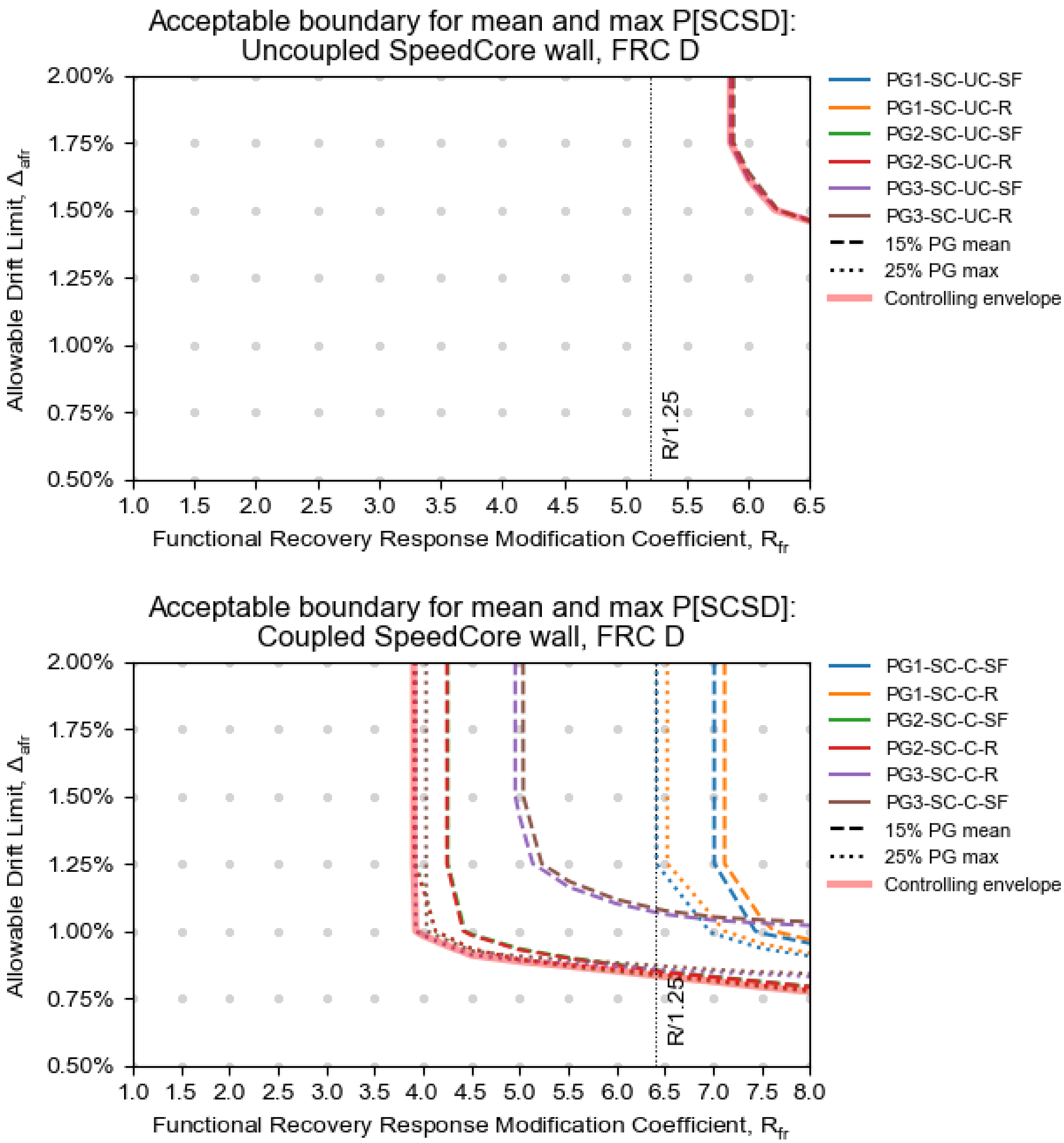

Figure 18 – Combination of R_{fr} and Δ_{afr} values required to satisfy the FRC D structural performance acceptance criteria for each performance group.

4.3. System Response

The figures below provide detailed insights into the general response and performance outcomes of the models making up each performance group. Figure 19 and Figure 20 show how design drift (Δ_{afr}) relates to median realized drift, and how realized drift relates to P[SCSD] for uncoupled and coupled performance groups, respectively. Breakdowns of the contributions of SCSD by structural component type are provided in Figure 21 and Figure 22 for uncoupled and coupled performance groups, respectively. Finally, Figure 23 shows when the building design transitions from strength-controlled to stiffness-controlled for various R_{fr} and Δ_{afr} combinations. All results presented in this section are general to the response of the system and not specific to Functional Recovery Category.

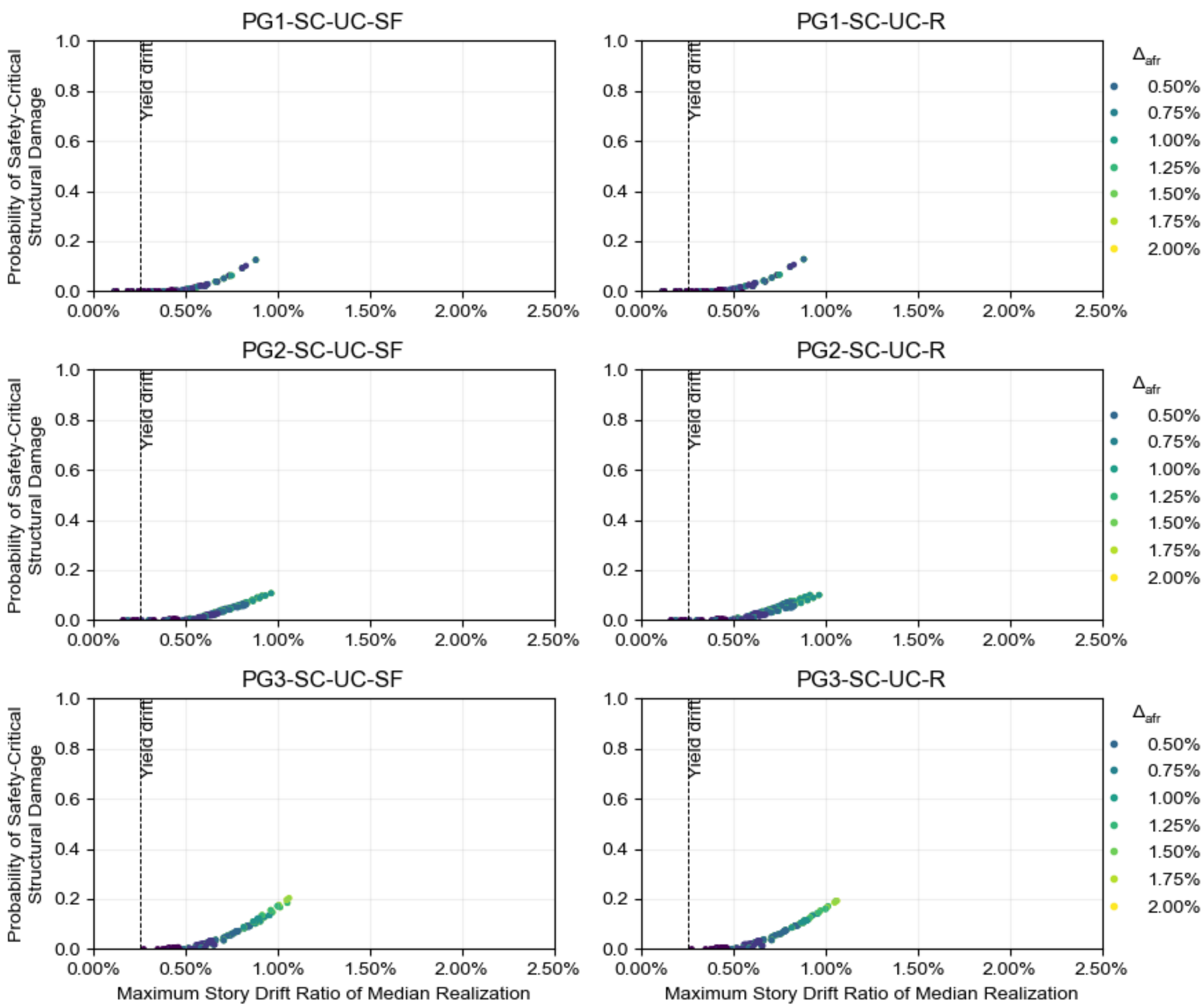

Figure 19 - Relationship between peak realized drift (median) and P[SCDS] for uncoupled archetypes

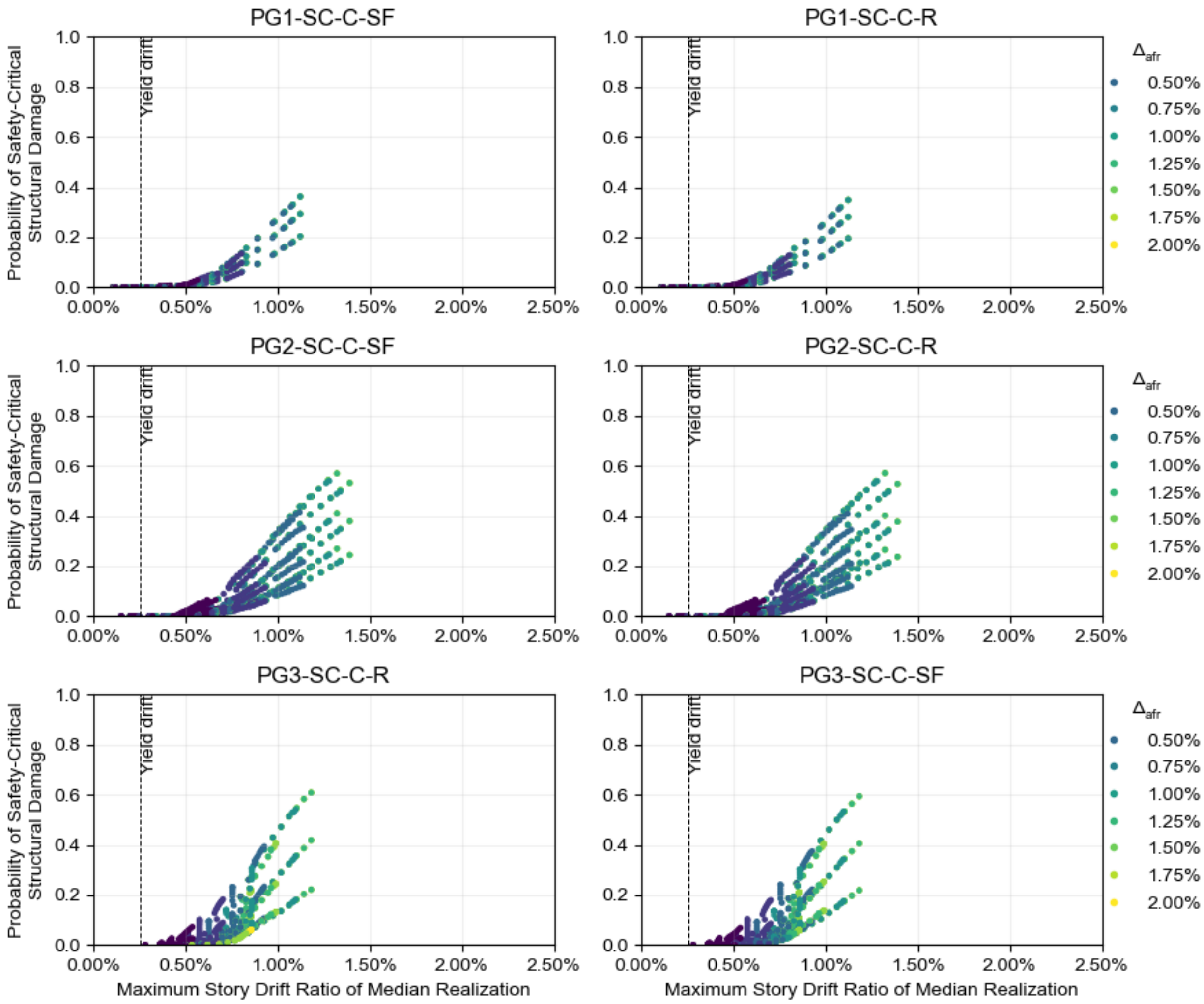

Figure 20 - Relationship between peak realized drift (median) and P[SCDS] for coupled archetypes

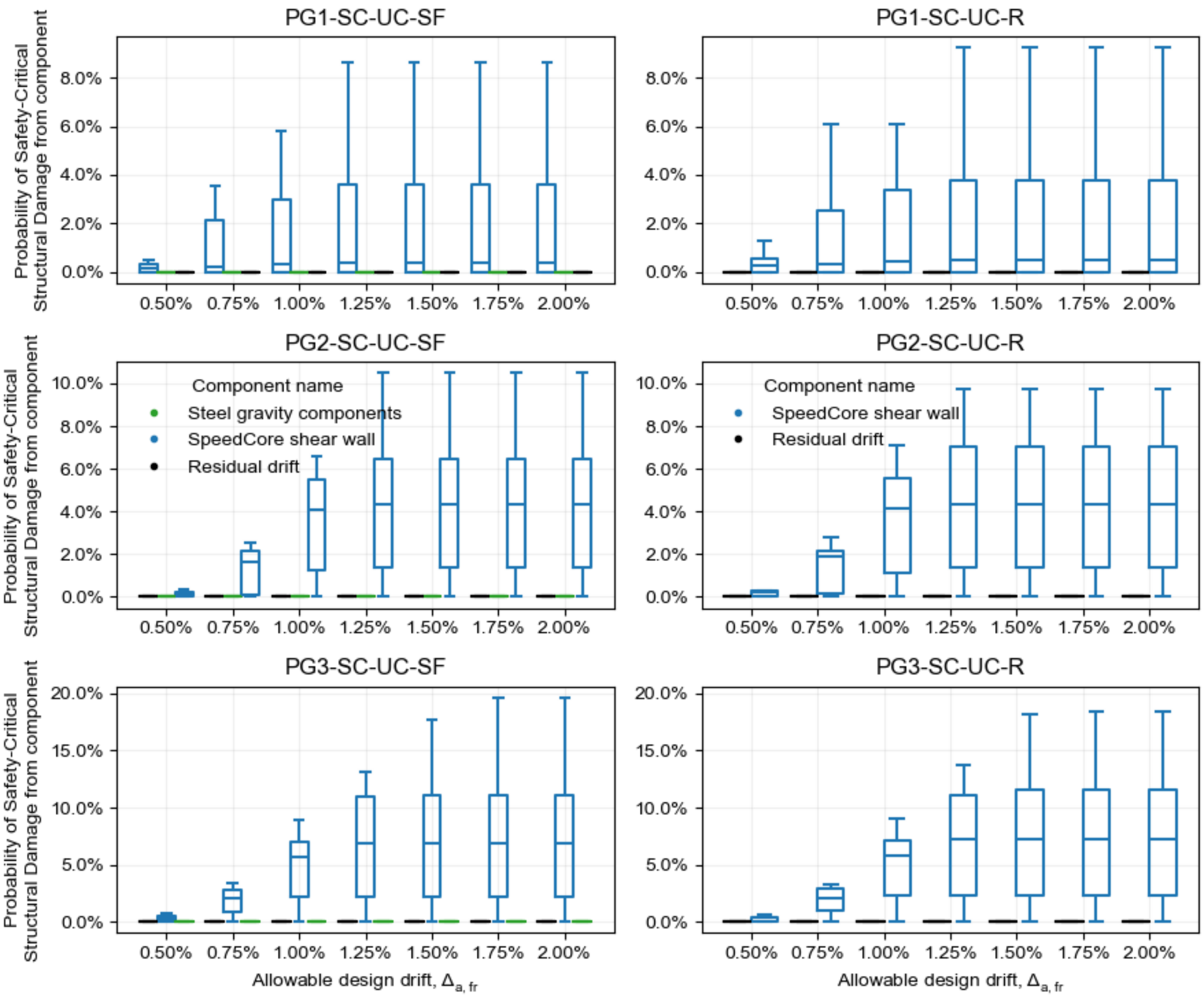

Figure 21 – Component damage contribution to P[SCSD] for uncoupled performance groups

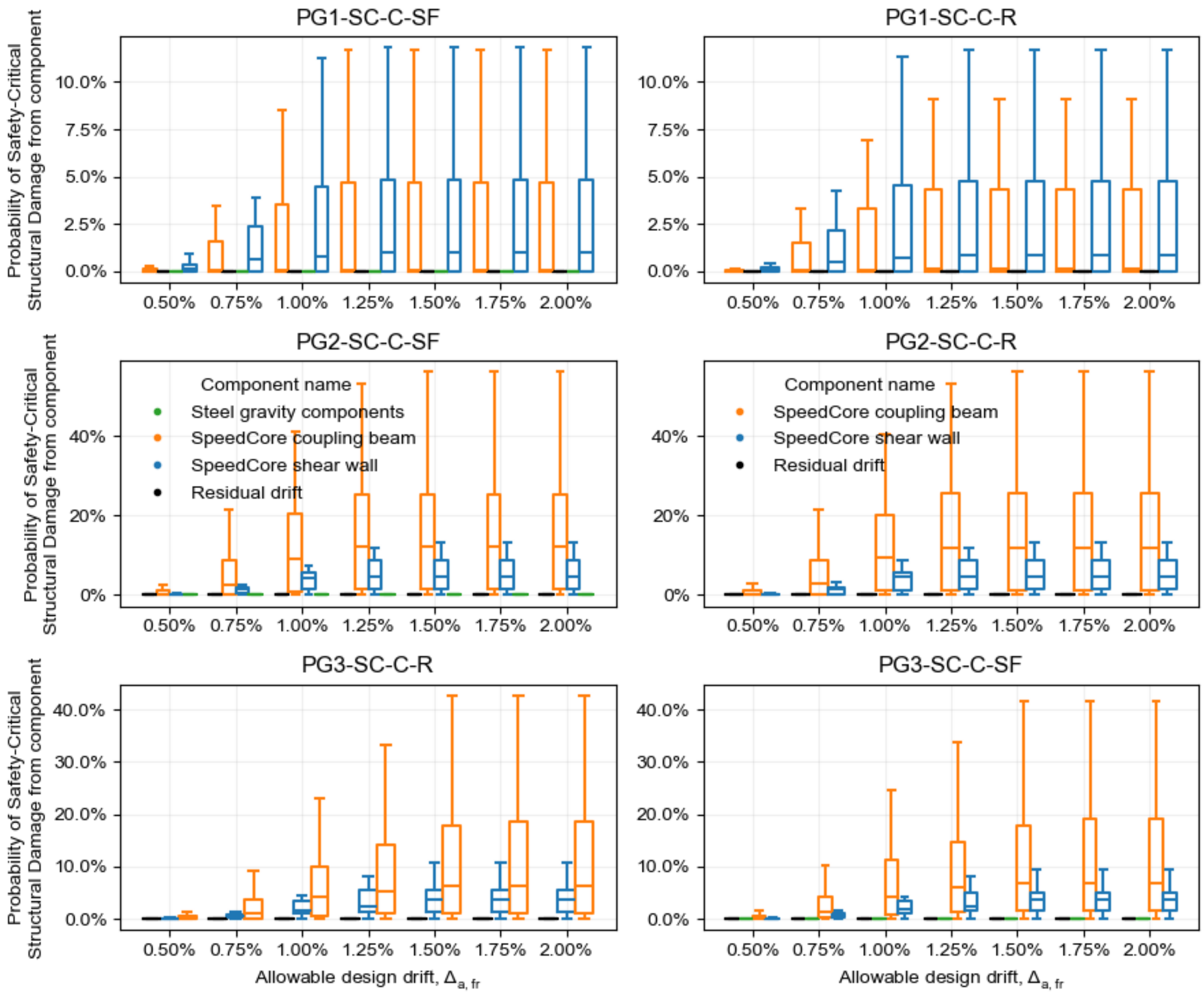

Figure 22 – Component damage contribution to P[SCSD] for coupled performance groups

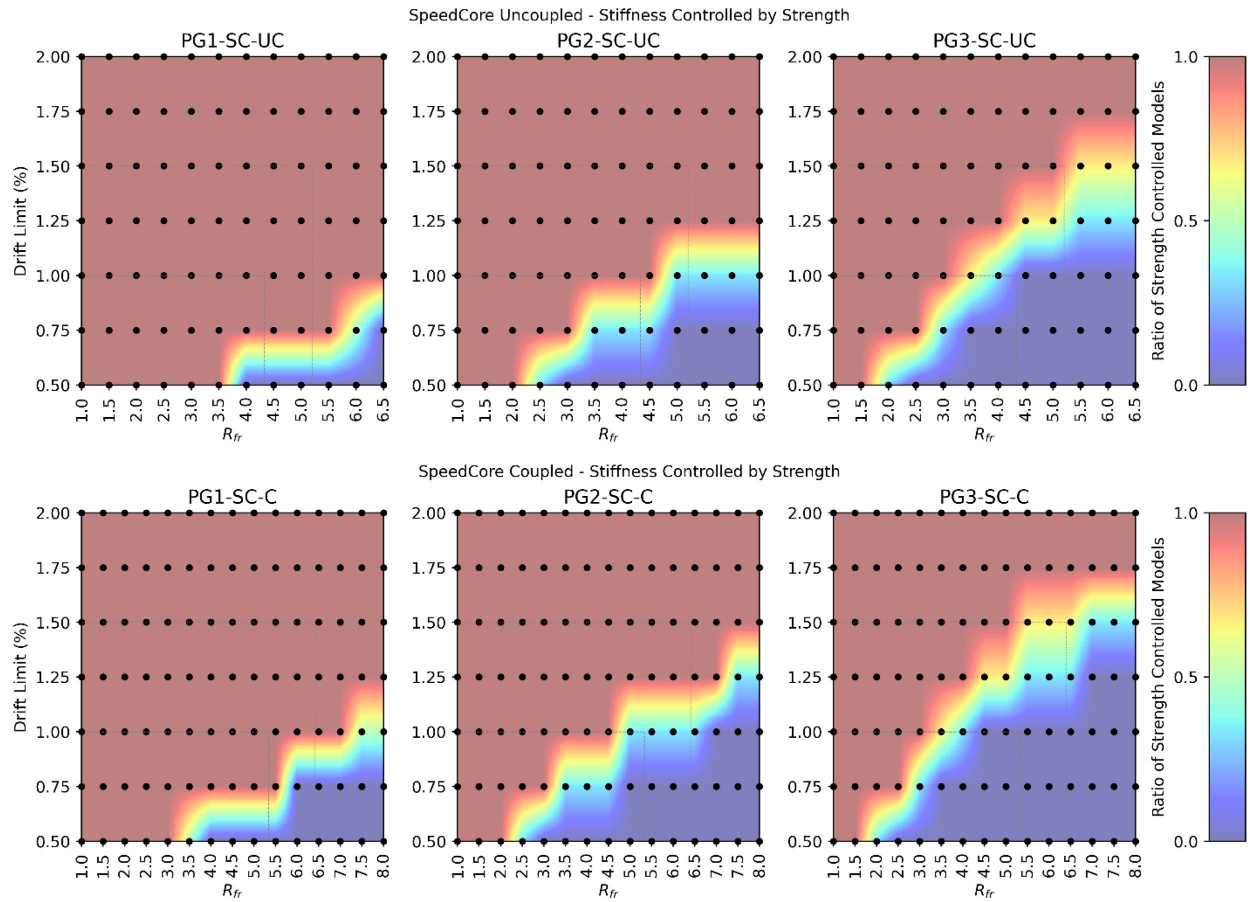

Figure 23 – Average influence of strength on building stiffness for various design requirement combinations assessed. Red coloring indicates that 100% of the models at this design point are controlled by strength requirements (e.g., tightening drift limits by one increment will not change performance). Alternately, blue coloring indicates that 100% of the models at this design point are controlled by stiffness requirements.

5. CONCLUSIONS

This report documents the quantification of the functional recovery seismic performance factors for the SpeedCore system in accordance with the proposed Section A.8 procedures of the 2026 National Earthquake Hazards Reduction Program (NEHRP) Provisions. The recommended functional recovery seismic performance factors, including the functional recovery response modification coefficient, R_{fr}, and functional recovery allowable story drift limit, Δ_{afr}., for the coupled and uncoupled SpeedCore wall systems are summarized in Table 15 and Table 16, respectively.

As shown in the previous sections, safety-critical structural damage in the SpeedCore archetypes was primarily driven by wall damage at the base for uncoupled systems and primarily controlled by coupling beam damage in the coupled systems (with some wall damage contributing, especially for the shorter archetypes). For the coupled systems, the results were very sensitive to coupling beam length, and SpeedCore coupled archetypes with the short, 6ft coupling beam, did not pass the prequalification without overly restrictive drift limits and R_{fr} values. Therefore, the 6ft coupling beam configurations are excluded from the recommended results in Table 15 and the recommended seismic performance factors are restricted to coupled SpeedCore systems with coupling beam lengths greater than or equal to 7.5ft in length.For all archetypes, the choice of allowable drift limits was informed by the independent strength and stiffness check, which indicated that the best balance point between drift limits and R_{fr} values corresponded to a 1.0% drift limit for uncoupled walls and a 0.75% drift limit for coupled walls. The final R_{fr} values were all dictated by the judgment-based limits, whereas the required drift limits were controlled primarily by the analysis results (at or below the judgment-based limits).

Table 15. Summary of functional recovery seismic performance factors for the coupled SpeedCore walls.

	FRC A/B/C		FRC D	
	R_{fr}	**Δ_{afr}**	**R_{fr}**	**Δ_{afr}**
Analysis results	6.5	0.75%*	8.0	0.75%*
Strength-stiffness independent check	5.5	0.75%	7.5	0.75%
Judgment-based upper limit	5.5	1.00%	6.5	1.50%
Recommendation – SpeedCore Coupled†	**5.5**	**0.75%**	**6.5**	**0.75%**

*Δ_{afr} of 0.75% was selected based on the performance envelope of the strength-and-stiffness-independent check, which indicated substantially better performance for coupled walls designed to less than 1.00% Δ_{afr}.

†Applicable to coupled SpeedCore systems with coupling beam lengths greater than or equal to 7.5ft in length.

Table 16. *Summary of functional recovery seismic performance factors for uncoupled SpeedCore walls.*

	FRC A/B/C		FRC D	
	R_{fr}	Δ_{afr}	R_{fr}	Δ_{afr}
Analysis result	6.5	1.00%*	6.5	1.00%*
Strength/stiffness independent check	6.5	1.00%	5.5	1.00%
Judgment-based upper limit	4.5	1.00%	5.0	1.50%
Recommendation – SpeedCore Uncoupled	**4.5**	**1.00%**	**5.0**	**1.00%**

* Δ_{afr} of 1.0% was selected on the performance envelope of the strength-and-stiffness-independent check, which indicated substantially better performance for low-rise uncoupled walls designed to less than 1.25% Δ_{afr}.

SUPPLEMENTARY MATERIAL

Two supplementary files are attached to this Prequalification Report that provide additional detailed information on the structural response and ATC 138 outcomes from individual archetype models and performance groups. The general description of the content contained in each file is provided below to assist with navigation and comprehension of detailed results.

- **Analysis Report Tables**
  SupplementalData_AnalysisReportTables_SpeedCore_final(v4_3c).xlsx
  - Contains detailed analysis outcomes for each archetype model assessed, including results for FRC A/B/C and FRC D.
  - “Summary” tab provides a summary of the controlling design values and other response metrics for each archetype
  - “All Runs” tab provides response and performance outcomes for all combinations of model runs for each archetype.
- **Archetype Performance Plots**
  SupplementalData_ArchtypePerformancePlotsAppendix_SpeedCore_final(v4_3c).pdf
  - Provides visualizations of analysis outcomes similar to the figures in the report, but for individual archetype models.
  - Provide peak drift and peak floor acceleration response profiles for each archetype model.

REFERENCES

Agrawal, S., Broberg, M., Varma, A.H. (2020). "Seismic Design Coefficients for SpeedCore or Composite Plate Shear Walls – Concrete Filled (C-PSW/CF)," Prepared for the Charles Pankow Foundation and the American Institute for Steel Construction, Purdue University, West Lafayette, IN.

AISC. (2022). "Seismic Provisions for Structural Steel Buildings," *ANSI/AISC 341-22*, American Institute of Steel Construction, Chicago, IL.

Ahmad, M., Shafaei, S., Bradt, T.G., Varma, A.H. (2021). "Seismic Design and Behavior of Composite Coupling Beam-to-C-PSW/CF Connections," Prepared for the Charles Pankow Foundation and American Institute of Steel Construction, Purdue University, West Lafayette, IN.

Ahmad, M., Shafaei, S., Varma, A.H., Klemencic, R. (2024). "Experimental Investigation of Composite Coupling Beam-to-Wall Connections in Coupled C-PSW/CF Systems," *Journal of Structural Engineering*, **150**(9): 04024114.

Almeter, E., Wade, K.F., Haselton, C.B., Saxey, B. (2018). "Rapid Risk Assessment of Buckling Restrained Braced Frames, With Focus on Residual Drifts," *Proceedings of the 11th U.S. National Conference on Earthquake Engineering* (11NCEE), Los Angeles, CA.

Almeter, E., DeBock, D.J., Haselton, C.B. (2024). *Structural Response Prediction Method for SpeedCore Buildings*, Prepared by Haselton Baker Risk Group for the American Institute for Steel Construction, Chicago, IL.

Alzeni, Y., Bruneau, M. (2014). "Cyclic Inelastic Behavior of Concrete Filled Sandwich Panel Walls Subjected to In-Plane Flexure," *Technical Report MCEER-14-0009*, University at Buffalo, Buffalo, NY.

Alzeni, Y., Bruneau, M. (2017). "In-Plane Cyclic Testing of Concrete-Filled Sandwich Steel Panel Walls with and without Boundary Elements," *Journal of Structural Engineering*, **143**(9): 04017115.

ASCE. (2022). "Minimum Design Loads and Associated Criteria for Buildings and Other Structures," *ASCE/SEI 7-22*, American Society of Civil Engineers, Reston, VA.

ATC. (2021). "Seismic Performance Assessment of Buildings: Volume 8 – Methodology for Assessment of Functional Recovery Time, *ATC-138-3*, Preliminary report for FEMA P-58-8, Prepared by the Applied Technology Council for the Federal Emergency Management Agency, Washington, DC.

Blowes, K., Molina-Hutt, C., Zimmerman, R., Cook, D.T., Almeter, E., Haselton, C.B. (2025). "Limiting Safety-Critical Structural Damage in Recovery-Based Seismic Design Provisions," *Earthquake Spectra* (manuscript under review).

Broberg, M., Agrawal, S., Varma, A.H., Klemencic, R. (2023). "Seismic design parameters (R, C_d, Ω_0) for uncoupled composite plate shear walls – concrete filled (C-PSW/CF)," *Earthquake Engineering and Structural Dynamics*, **52**: 3149-3170.

Bruneau, M., Varma, A.H., Kizlarslan, E., Broberg, M., Shafaei, S., Seo, J. (2019). "R-Factors for Coupled Composite Plate Shear Walls/Concrete Filled (CC-PSW/CF)," Prepared for the Charles Pankow Foundation and the American Institute for Steel Construction, University at Buffalo (Buffalo, NY) and Purdue University (West Lafayette, IN).

Cook, D., Wade, K., Haselton, C., Baker, J. W., & DeBock, D. J. (2018). A structural response prediction engine to support advanced seismic risk assessment. In Eleventh US national conference on earthquake engineering, Los Angeles, CA.

DeBock, D., Manousakis, I.V., Deierlein, G.G., Zsarnóczay, A. (2024). "Updated Model and Criteria for Residual Drift," *FEMA P-58/BD-3.7.26*, Background documentation for the ATC-138/FEMA P-58 Project, Submitted to the Applied Technology Council, Prepared for the Federal Emergency Management Agency, Washington, DC.

Deierlein, G., Victorsson, V. (2008). "Fragility Curves for Components of Steel SMF Systems," FEMA P-58/BD-3.8.3, Background document for the FEMA P-58 project, Submitted to the Applied Technology Council and Prepared for the Federal Emergency Management Agency, Washington, DC.

FEMA. (2009). "Quantification of Building Seismic Performance Factors," *FEMA P695*, Prepared by the Applied Technology Council for the Federal Emergency Management Agency, Washington, DC.

FEMA. (2018a). "Seismic Performance Assessment of Buildings: Volume 1 – Methodology," *FEMA P-58-1*, 2nd Edition, Prepared by the Applied Technology Council for the Federal Emergency Management Agency, Washington, DC.

FEMA. (2018b). "Seismic Performance Assessment of Buildings: Volume 2 – Implementation Guide," *FEMA P-58-2*, 2nd Edition, Prepared by the Applied Technology Council for the Federal Emergency Management Agency, Washington, DC.

Haselton Baker Risk Group (2025). Seismic Performance Prediction Program (SP3).

Kenarangi, H., Kizilarslan, E., Polat, E., Bruneau, M. (2020). "Cyclic Inelastic Behavior of C-Shaped Composite Plate Shear Walls-Concrete Filled (C-PSW/CF) Walls," Prepared for the Charles Pankow Foundation and American Institute of Steel Construction, University at Buffalo, Buffalo, NY.

Kenarangi, H., Kizilarslan, E., Bruneau, M., (2021). "Cyclic Behavior of C-Shaped Composite Plate Shear Walls - Concrete Filled," *Engineering Structures*, **226**(1): 111306.

Kizilarslan, E., Kenarangi, H., Bruneau, M. (2021a). "Cyclic Inelastic Behavior of T-Shaped Composite Plate Shear Walls-Concrete Filled (C-PSW/CF)," Prepared for the Charles

Pankow Foundation and American Institute of Steel Construction, University at Buffalo, Buffalo, NY.

Kizilarslan, E., Broberg, M., Shafaei, S., Varma, A.H., Bruneau, M. (2021b). "Seismic design coefficients and factors for coupled composite plate shear walls/concrete filled (CC-PSW/CF)," *Engineering Structures*, **244**: 112766.

Kizilarslan, E., Bruneau, M., (2023a). "Cyclic Behavior of T-Shaped Concrete Filled-Composite Plate Shear Walls (CF CPSWs)," *Journal of Structural Engineering*, **149**(8): 04023102.

Kizilarslan E., Bruneau, M., (2023b). "Verification of Seismic Response Modification Factors of Uncoupled Composite Plate Shear Walls/concrete-filled (C-PSW/CF)," *Journal of Structural Engineering*, **149**(6): 04023060.

Liu, J., Astaneh-Asl, A. (2000). "Cyclic testing of simple connections including effects of slab," *Journal of Structural Engineering*, **126**(1): 32-39.

McKenna, F., Scott, M.H., Fenves, G.L. (2010). "Nonlinear Finite-Element Analysis Software Architecture using Object Composition," *Journal of Computing in Civil Engineering*, **24**(1): 95-107.

Miranda, E. (1999). "Approximate seismic lateral deformation demands in multistory buildings," *Journal of Structural Engineering*, **125**(4): 417-425.

Miranda, E., Reyes, C.J. (2002). "Approximate lateral drift demands in multistory buildings with nonuniform stiffness," *Journal of Structural Engineering*, **128**(7): 840-849.

Shafaei, S., Seo, J., Varma, A.H. (2020). "Experimental Evaluation of Planar Composite Plate Shear Walls/Concrete Filled (SpeedCore)," Prepared for the Charles Pankow Foundation and American Institute of Steel Construction, Purdue University, West Lafayette, IN.

Shafaei, S., Varma, A.H., Seo, J., Klemencic, R. (2021). "Cyclic Lateral Loading Behavior of Composite Plate Shear Walls/Concrete Filled," *Journal of Structural Engineering*, **147**(10): 04021145.

Tauberg, N.A., Kolozvari, K., Wallace, J.W. (2019). "Ductile Reinforced Concrete Coupled Walls: FEMA P695 Study," *Report UCLA SEERL 2019/01*, University of California, Los Angeles.

Vamvatsikos, D., Cornell, C.A. (2002). "Incremental Dynamic Analysis," *Earthquake Engineering and Structural Dynamics*, **31**(3): 491-514.

Varma, A.H., Broberg, M., Shafaei, S., Taghipour, A.A. (2023). "SpeedCore Systems for Steel Structures," AISC Design Guide 38, American Institute for Steel Construction, Chicago, IL.

Vouvakis Manousakis I., Zsarnoczay A., Konstantinidis D., (2024), "Robust Residual Drift Estimation for Seismic Performance Assessment based on High-Fidelity Response Simulation of Steel Frames," (manuscript in preparation).

Welch, D.P., Almeter, E., DeBock, D.J., Haselton, C.B. (2024). FEMA P-58 Fragility Function Development for the SpeedCore Wall System, Prepared by Haselton Baker Risk Group for the American Institute for Steel Construction, Chicago, IL.

White, T., Adebar, P. (2004). "Estimating Rotational Demands in High-Rise Concrete Wall Buildings," *Proceedings of the 13th World Conference on Earthquake Engineering*, Vancouver, Canada.